Statically Determinate Plane Frames

4

Abstract

Plane frame structures are composed of structural members which lie in a single plane. When loaded in this plane, they are subjected to both bending and axial action. Of particular interest are the shear and moment distributions for the members due to gravity and lateral loadings. We describe in this chapter analysis strategies for typical statically determinate single-story frames. Numerous examples illustrating the response are presented to provide the reader with insight as to the behavior of these structural types. We also describe how the Method of Virtual Forces can be applied to compute displacements of frames. The theory for frame structures is based on the theory of beams presented in Chap. 3. Later in Chaps. 9, 10, and 15, we extend the discussion to deal with statically indeterminate frames and space frames.

4.1 Definition of Plane Frames

The two dominant planar structural systems are plane trusses and plane frames. Plane trusses were discussed in detail in Chap. 2. Both structural systems are formed by connecting structural members at their ends such that they are in a single plane. The systems differ in the way the individual members are connected and loaded. Loads are applied at nodes (joints) for truss structures. Consequently, the member forces are purely axial. Frame structures behave in a completely different way. The loading is applied directly to the members, resulting in internal shear and moment as well as axial force in the members. Depending on the geometric configuration, a set of members may experience predominately bending action; these members are called "beams." Another set may experience predominately axial action. They are called "columns." The typical building frame is composed of a combination of beams and columns.

Frames are categorized partly by their geometry and partly by the nature of the member/member connection, i.e., pinned vs. rigid connection. Figure 4.1 illustrates some typical rigid plane frames used mainly for light manufacturing factories, warehouses, and office buildings. We generate three-dimensional frames by suitably combining plane frames.

J.J. Connor, S. Faraji, *Fundamentals of Structural Engineering*,
DOI 10.1007/978-3-319-24331-3_4

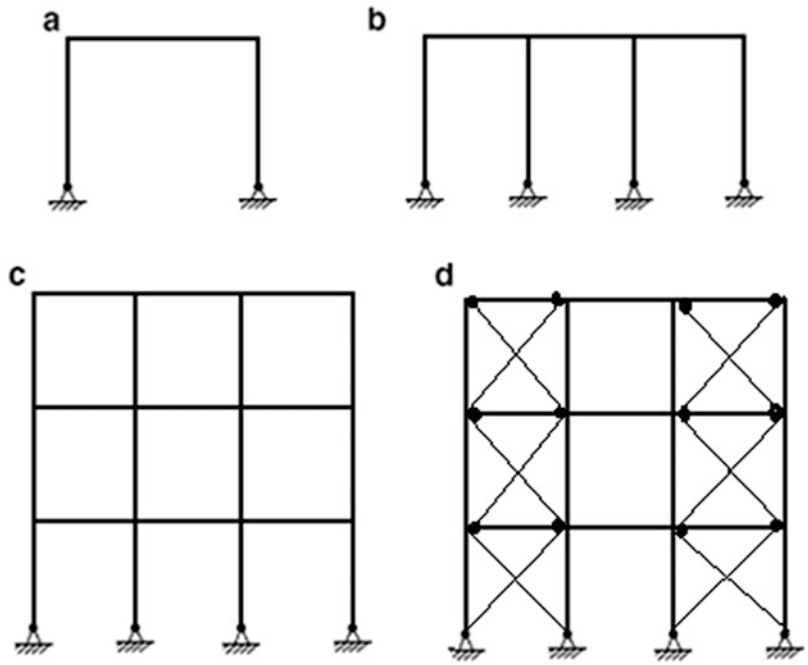

Fig. 4.1 Typical plane building frames. (**a**) Rigid portal frame. (**b**) Rigid multi-bay portal frame. (**c**) Multistory rigid frame. (**d**) Multistory braced frame

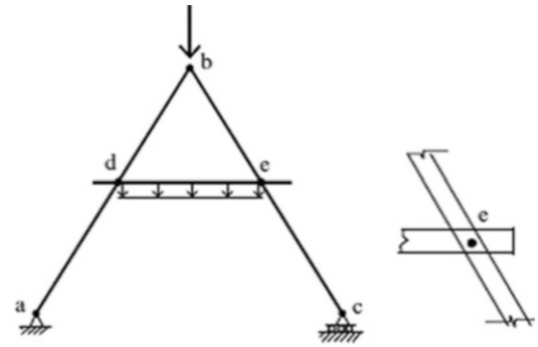

Fig. 4.2 A-frame

Figure 4.2 shows an A-frame, named obviously for its geometry. This frame has three members ab, bc, and de that are pinned together at points d, b, and e. Loads may be applied at the connection points, such as b, or on a member, such as de. A-frames are typically supported at the base of their legs, such as at a and c. Because of the nature of the loading and restraints, the members in an A-frame generally experience bending as well as axial force.

To provide more vertical clearance in the interior of the portal frame, and also to improve the aesthetics, a more open interior space is created by pitching the top member as illustrated in Fig. 4.3. Pitched roof frames are also referred to as gable frames. Architects tend to prefer them for churches, gymnasia, and exhibition halls.

4.2 Statical Determinacy: Planar Loading

All the plane frames that we have discussed so far can be regarded as rigid bodies in the sense that if they are adequately supported, the only motion they will experience when a planar load is applied will

Fig. 4.3 Gable (pitched roof) frames

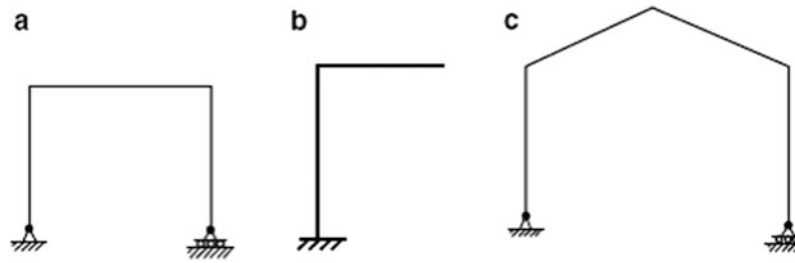

Fig. 4.4 Statically determinate support schemes for planar frames

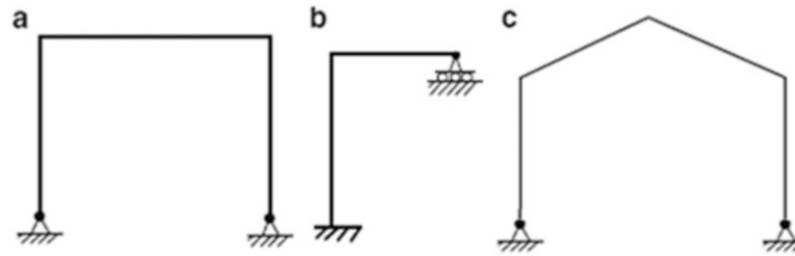

Fig. 4.5 Statically indeterminate support schemes—planar frames

be due to deformation of the members. Therefore, we need to support them with only three nonconcurrent displacement restraints. One can use a single, fully fixed support scheme, or a combination of hinge and roller supports. Examples of "adequate" support schemes are shown in Fig. 4.4. All these schemes are statically determinate. In this case, one first determines the reactions and then analyzes the individual members.

If more than three displacement restraints are used, the plane frames are statically indeterminate. In many cases, two hinge supports are used for portal and gable frames (see Fig. 4.5). We cannot determine the reaction forces in these frame structures using only the three available equilibrium equations since there are now four unknown reaction forces. They are reduced to statically determinate structures by inserting a hinge which acts as a moment release. We refer to these modified structures as 3-hinge frames (see Fig. 4.6).

Statical determinacy is evaluated by comparing the number of unknown forces with the number of equilibrium equations available. For a planar member subjected to planar loading, there are three internal forces: axial, shear, and moment. Once these force quantities are known at a point, the force quantities at any other point in the member can be determined using the equilibrium equations. Figure 4.7 illustrates the use of equilibrium equations for the member segment AB. Therefore, it follows that there are only *three force unknowns for each member* of a rigid planar frame subjected to planar loading.

We define a node (joint) as the intersection of two or more members, or the end of a member connected to a support. A node is acted upon by member forces associated with the members' incident on the node. Figure 4.8 illustrates the forces acting on node B.

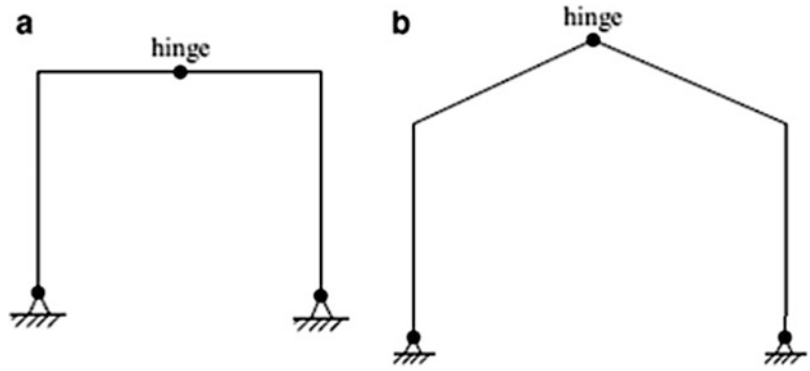

Fig. 4.6 3-Hinge plane frames

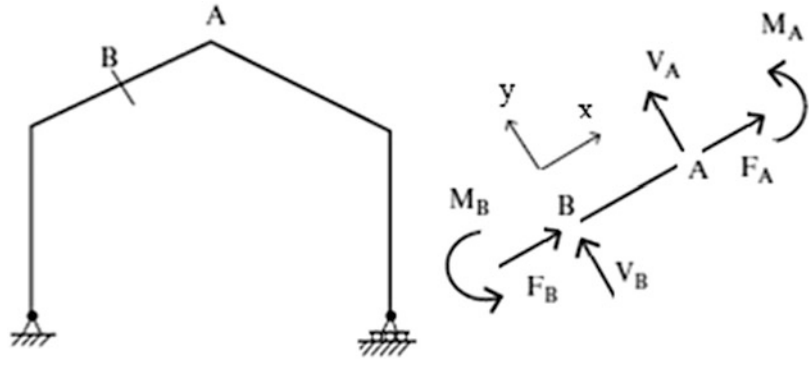

Fig. 4.7 Free body diagram—member forces

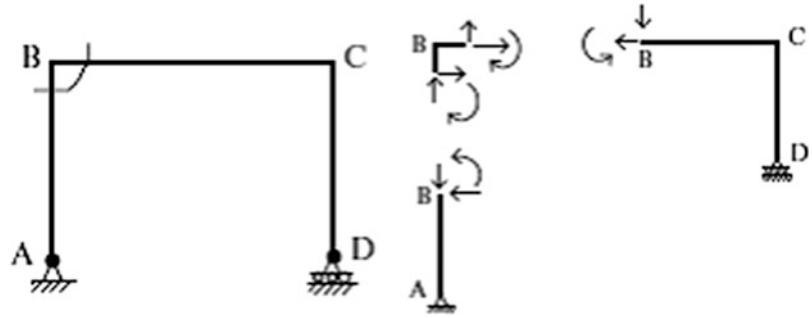

Fig. 4.8 Free body diagram—node B

These nodal forces comprise a general planar force system for which there are three equilibrium equations available; summation of forces in two nonparallel directions and summation of moments. Summing up force unknowns, we have three for each member plus the number of displacement restraints. Summing up equations, there are three for each node plus the number of force releases (e.g., moment releases) introduced. Letting m denote the number of members, r the number of

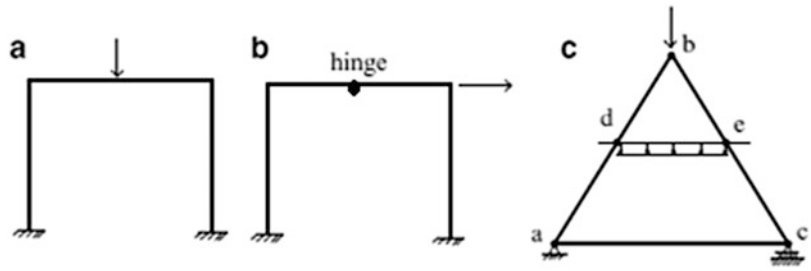

Fig. 4.9 Indeterminate portal and A-frames

displacement restraints, j the number of nodes, and n the number of releases, the criterion for statical determinacy of *rigid plane frames* can be expressed as

$$3m + r - n = 3j \tag{4.1}$$

We apply this criterion to the portal frames shown in Figs. 4.4a, 4.5a, and 4.6b. For the portal frame in Fig. 4.4a

$$m = 3, \quad r = 3, \quad j = 4$$

For the corresponding frame in Fig. 4.5a

$$m = 3, \quad r = 4, \quad j = 4$$

This structure is indeterminate to the first degree. The 3-hinge frame in Fig. 4.6a has

$$m = 4, \quad r = 4, \quad n = 1, \quad j = 5$$

Inserting the moment release reduces the number of unknowns and now the resulting structure is statically determinate.

Consider the plane frames shown in Fig. 4.9. The frame in Fig. 4.9a is indeterminate to the third degree.

$$m = 3, \quad r = 6, \quad j = 4$$

The frame in Fig. 4.9b is indeterminate to the second degree.

$$m = 4, \quad r = 6, \quad j = 5 \quad n = 1$$

Equation (4.1) applies to rigid plane frames, i.e., where the members are rigidly connected to each other at nodes. The members of an A-frame are connected with pins that allow relative rotation and therefore A-frames are *not* rigid frames. We establish a criterion for A-frame type structures following the same approach described above. Each member has three equilibrium equations. Therefore, the total number of equilibrium equations is equal to $3m$. Each pin introduces two force unknowns. Letting n_p denote the number of pins, the total number of force unknowns is equal to $2n_p$ plus the number of displacement restraints. It follows that

$$2n_p + r = 3m \tag{4.2}$$

for static determinacy of A-frame type structures. Applying this criterion to the structure shown in Fig. 4.2, one has $n_p = 3$, $r = 3$, $m = 3$, and the structure is statically determinate. If we add another member at the base, as shown in Fig. 4.9c, $n_p = 5$, $r = 3$, $m = 4$, and the structure becomes statically indeterminate to the first degree.

4.3 Analysis of Statically Determinate Frames

In this section, we illustrate with numerous examples the analysis process for statically determinate frames such as shown in Fig. 4.10a. In these examples, our primary focus is on the generation of the internal force distributions. Of particular interest are the location and magnitude of the peak values of moment, shear, and axial force since these quantities are needed for the design of the member cross sections.

The analysis strategy for these structures is as follows. We first find the reactions by enforcing the global equilibrium equations. Once the reactions are known, we draw free body diagrams for the members and determine the force distributions in the members. *We define the positive sense of bending moment according to whether it produces compression on the exterior face*. The sign conventions for bending moment, transverse shear, and axial force are defined in Fig. 4.10b.

The following examples illustrate this analysis strategy. Later, we present analytical solutions which are useful for developing an understanding of the behavior.

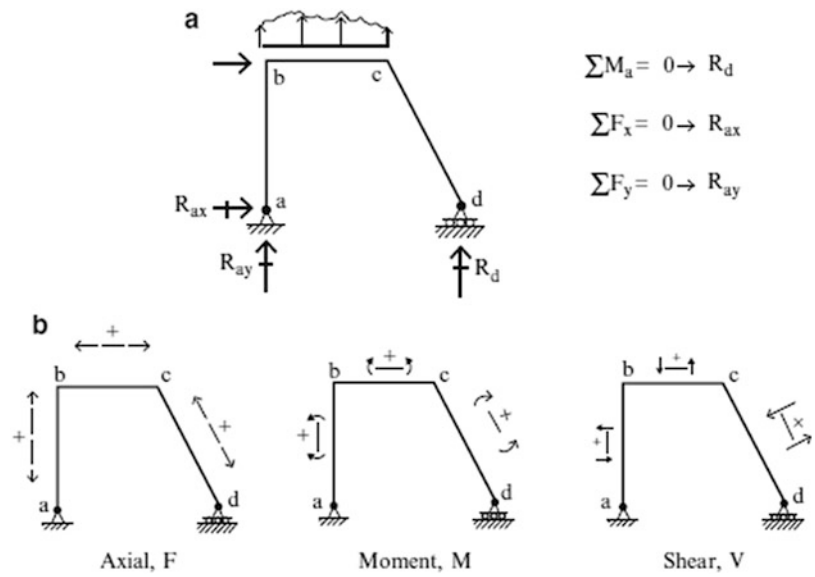

Fig. 4.10 (**a**) Typical frame. (**b**) Sign convention for the bending moment, transverse shear, and axial force

Example 4.1 UnsymmetricalCantilever Frame

Given: The structure defined in Fig. E4.1a.

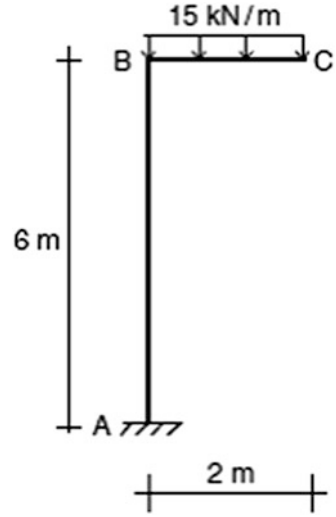

Fig. E4.1a

Determine: The reactions and draw the shear and moment diagrams.

Solution: We first determine the reactions at A, and then the shear and moment at B. These results are listed in Figs. E4.1b and E4.1c. Once these values are known, the shear and moment diagrams for members CB and BA can be constructed. The final results are plotted in Fig. E4.1d.

$$\begin{aligned}
\sum F_x &= 0 \quad R_{Ax} = 0 \\
\sum F_y &= 0 \quad R_{Ay} - (15)(2) = 0 \qquad R_{Ay} = 30\,\text{kN} \uparrow \\
\sum M_A &= 0 \quad M_A - (15)(2)(1) = 0 \qquad M_A = 30\,\text{kN m counter clockwise}
\end{aligned}$$

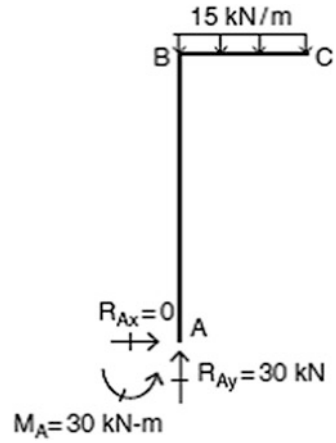

Fig. E4.1b Reactions

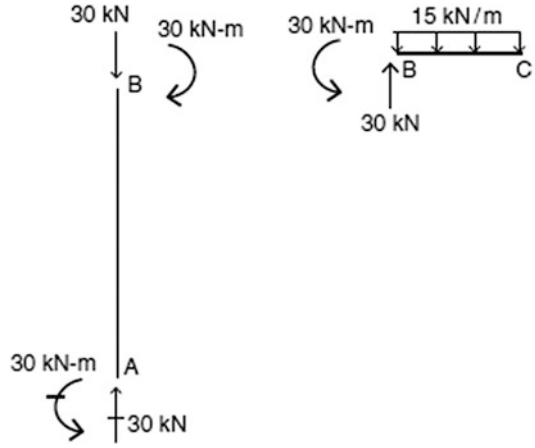

Fig. E4.1c End actions

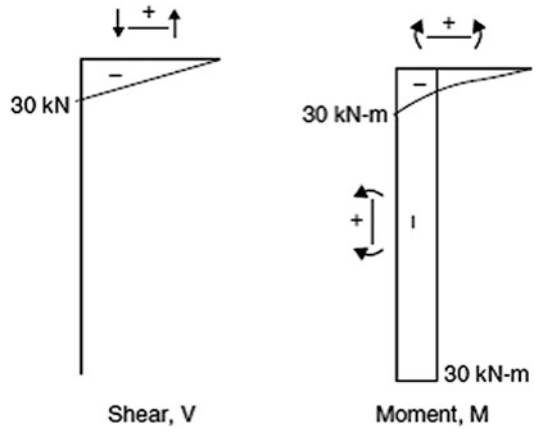

Fig. E4.1d Shear and moment diagrams

Example 4.2 Symmetrical Cantilever Frame

Given: The structure defined in Fig. E4.2a.

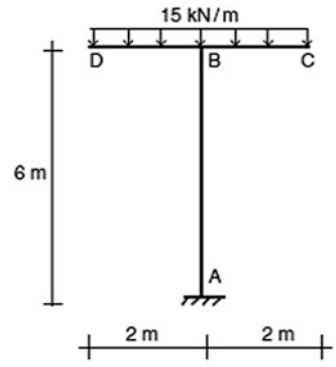

Fig. E4.2a

Determine: The reactions and draw the shear and moment diagrams.

Solution: We determine the reactions at A and shear and moment at B. The results are shown in Figs. E4.2b and E4.2c.

$$\begin{array}{lll} \sum F_x = 0 & R_{Ax} = 0 & \\ \sum F_y = 0 & R_{Ay} - (15)(4) = 0 & R_{Ay} = 60\,\text{kN} \uparrow \\ \sum M_A = 0 & M_A - (15)(2)(1) + (15)(2)(1) = 0 & M_A = 0 \end{array}$$

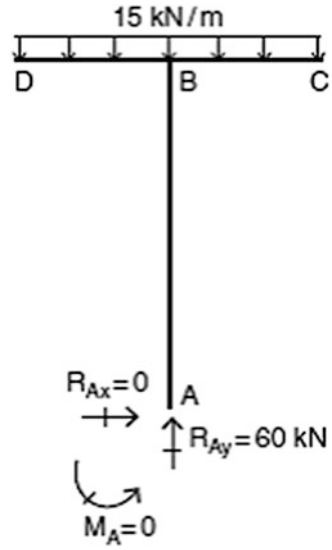

Fig. E4.2b Reactions

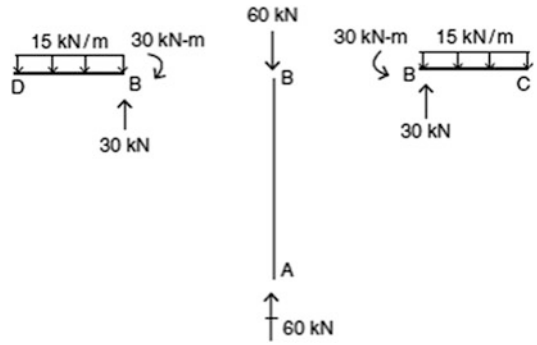

Fig. E4.2c End actions

Finally, the shear and moment diagrams for the structures are plotted in Fig. E4.2d. Note that member AB now has no bending moment, just axial compression of 60 kN.

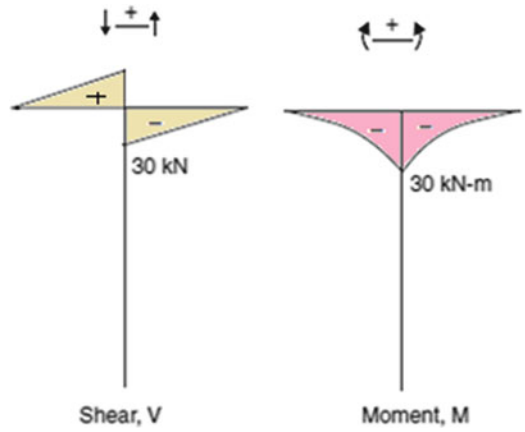

Fig. E4.2d Shear and moment diagrams

Example 4.3 Angle-Type Frame Segment

Given: The frame defined in Fig. E4.3a.

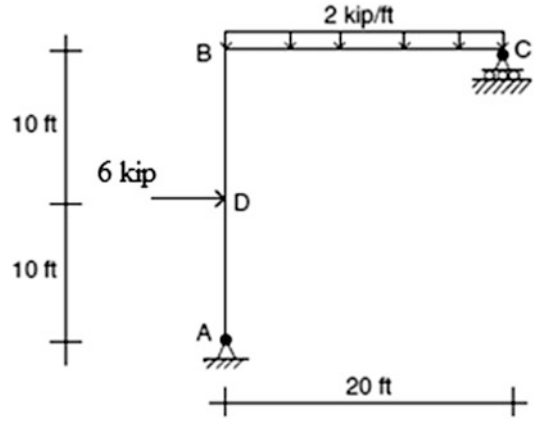

Fig. E4.3a

Determine: The reactions and draw the shear and moment diagrams.

Solution: We determine the vertical reaction at C by summing moments about A. The reactions at A follow from force equilibrium considerations (Fig. E4.3b).

$$\sum M_A = 0 \quad 2(20)(10) + 6(10) - R_C(20) = 0 \quad R_C = 23\,\text{kip} \uparrow$$
$$\sum F_x = 0 \quad R_{Ax} = 6\,\text{kip} \leftarrow$$
$$\sum F_y = 0 \quad R_{Ay} - 2(20) + 23 = 0 \quad R_{Ay} = 17\,\text{kip} \uparrow$$

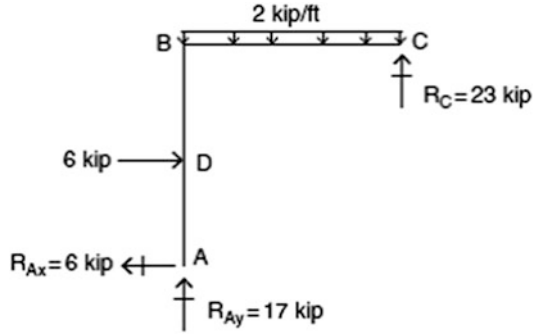

Fig. E4.3b Reactions

Next, we determine the end moments and end shears for segments CB and BA using the equilibrium equations for the members. Figure E4.3c contains these results.

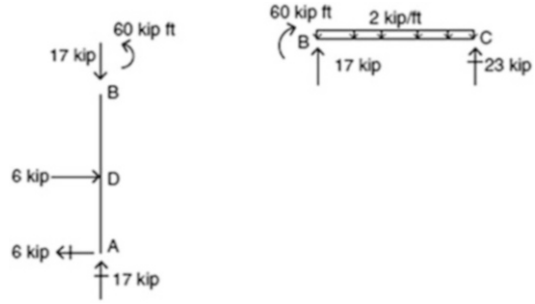

Fig. E4.3c End actions

Lastly, we generate the shear and bending moment diagrams (Fig. E4.3d). The maximum moment occurs in member BC. We determine its location by noting that the moment is maximum when the shear is zero.

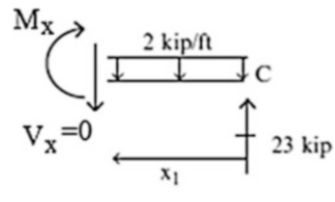

$$23 - (2)x_1 = 0 \rightarrow x_1 = 11.5\,\text{ft}$$

Then, $M_{\max} = 23(11.5) - \dfrac{2(11.5)^2}{2} = 132.25\,\text{kip ft}$

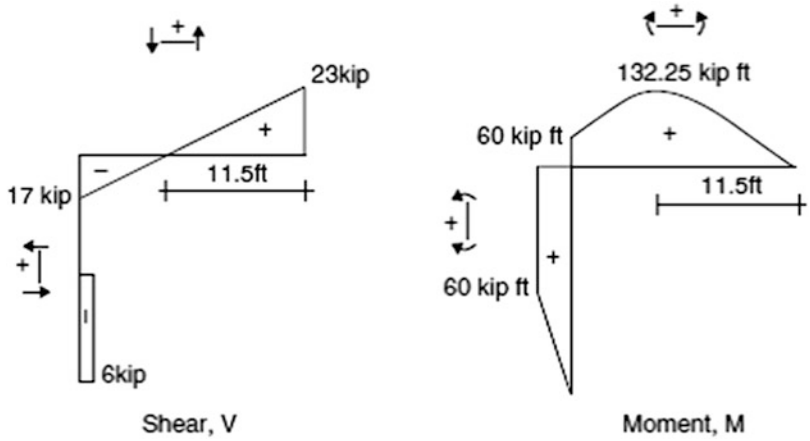

Fig. E4.3d Shear and moment diagrams

Example 4.4 Simply Supported Portal Frame

Given: The portal frame defined in Fig. E4.4a.

Determine: The shear and moment distributions.

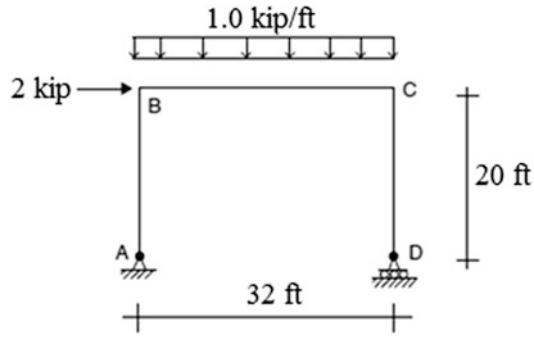

Fig. E4.4a

Solution: The reaction at D is found by summing moments about A. We then determine the reactions at A using force equilibrium considerations. Figure E4.4b shows the result.

$$\sum M_A = 0 \quad 1(32)(16) + 2(20) - R_D(32) = 0 \quad R_D = 17.25 \uparrow$$
$$\sum F_x = 0 \quad R_{Ax} = 2 \leftarrow$$
$$\sum F_y = 0 \quad R_{Ay} - 1(32) + 17.25 = 0 \quad R_{Ay} = 14.75 \uparrow$$

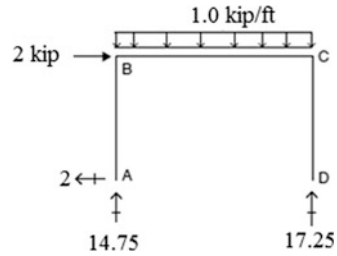

Fig. E4.4b Reactions

Isolating the individual members and enforcing equilibrium leads to the end forces and moments shown in Fig. E4.4c.

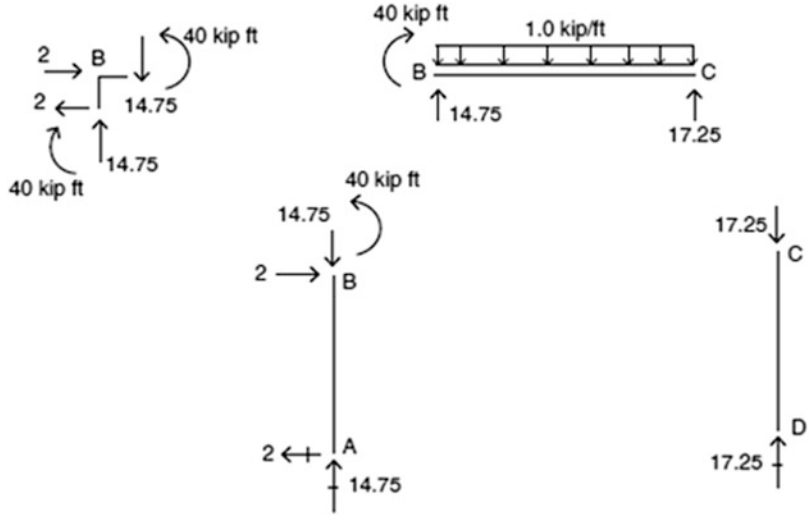

Fig. E4.4c End actions

We locate the maximum moment in member BC. Suppose the moment is a maximum at $x = x_1$. Setting the shear at this point equal to zero leads to

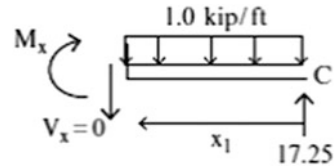

$$17.25 - x_1(1) = 0 \rightarrow x_1 = 17.25\,\text{ft}$$

Then, $M_{\max} = 17.25(17.25) - \dfrac{(1)(17.25)^2}{2} = 148.78\,\text{kip ft}$

The shear and moment diagrams are plotted in Fig. E4.4d.

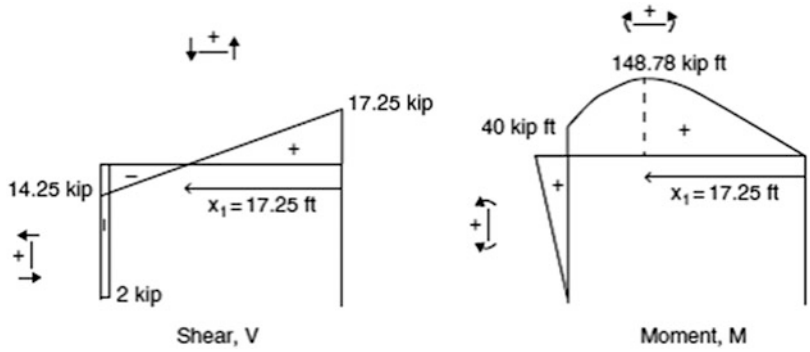

Fig. E4.4d Shear and moment diagrams

Example 4.5 3-Hinge Portal Frame

Given: The 3-hinge frame defined in Fig. E4.5a.

Determine: The shear and moment distributions.

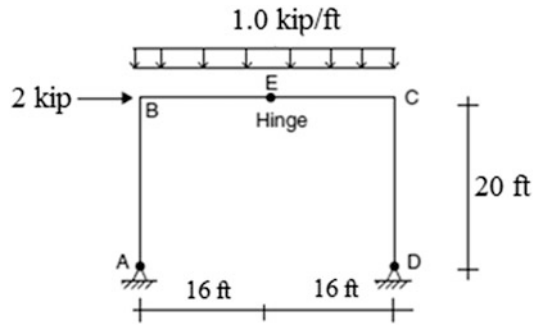

Fig. E4.5a

Solution: Results for the various analysis steps are listed in Figs. E4.5b, E4.5c, E4.5d, E4.5e, E4.5f, and E4.5g.

Step 1: Reactions at D and A

The vertical reaction at D is found by summing moments about A.

$$\sum M_{\mathrm{A}} = 0 \quad R_{\mathrm{D}y}(32) - (1)(32)(16) - 2(20) = 0 \quad R_{\mathrm{D}y} = 17.25\,\mathrm{kip} \uparrow$$

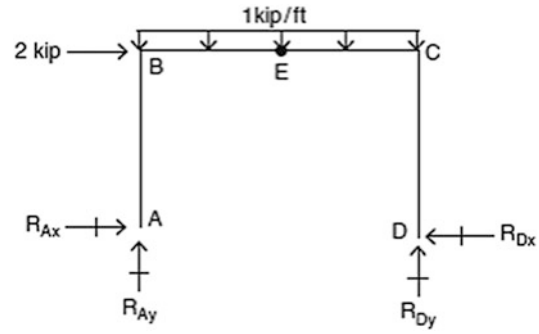

Fig. E4.5b

Next, we work with the free body diagram of segment ECD. Applying the equilibrium conditions to this segment results in

$$\sum M_{\mathrm{E}} = 0 \quad 17.25(16) - (1)(16)(8) - R_{\mathrm{DX}}(20) = 0 \quad R_{\mathrm{DX}} = 7.4\,\mathrm{kip} \leftarrow$$
$$\sum F_x = 0 \quad F_{\mathrm{E}} = -R_{\mathrm{DX}} = 7.4\,\mathrm{kip} \rightarrow$$
$$\sum F_y = 0 \quad -V_{\mathrm{E}} + 17.25 - (1)(16) = 0 \qquad V_{\mathrm{E}} = 1.25\,\mathrm{kip} \downarrow$$

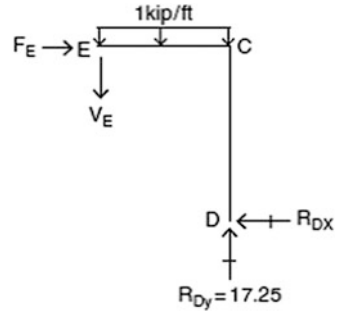

Fig. E4.5c

With the internal forces at E known, we can now proceed with the analysis of segment ABE.

$$\sum F_x = 0 \quad R_{Ax} + 2 - 7.4 = 0 \qquad R_{Ax} = 5.4\,\text{kip} \rightarrow$$
$$\sum F_y = 0 \quad R_{Ay} + 17.25 - (1)(32) = 0 \qquad R_{Ay} = 14.75\,\text{kip} \uparrow$$

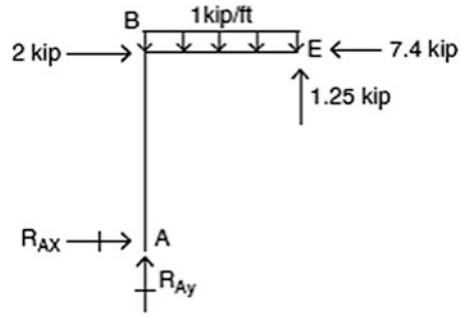

Fig. E4.5d

Reactions are listed below

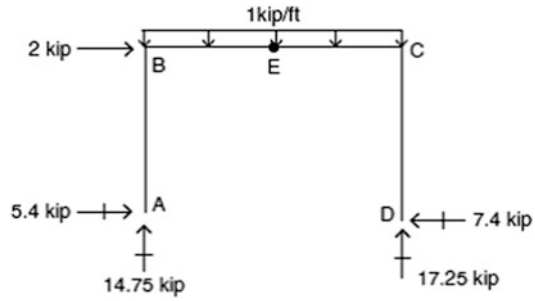

Fig. E4.5e Reactions

Step 2: End actions at B and C

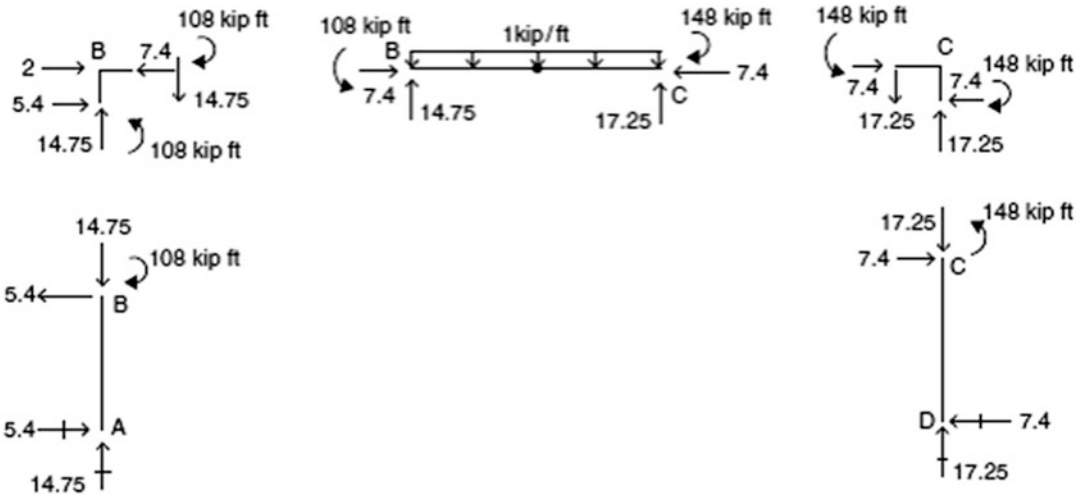

Fig. E4.5f End actions

Step 3: Shear and moment diagrams

First, we locate the maximum moment in member BC.

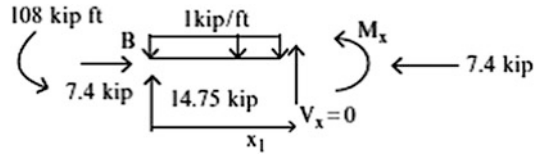

$$14.75 - (1)x_1 = 0 \rightarrow x_1 = 14.75\,\text{ft}$$

Then, $M_{\max} = 14.75(14.75) - \dfrac{1(14.75)^2}{2} - 108 = 0.78\,\text{kip ft}$

The corresponding shear and moment diagrams are listed in Fig. E4.5g.

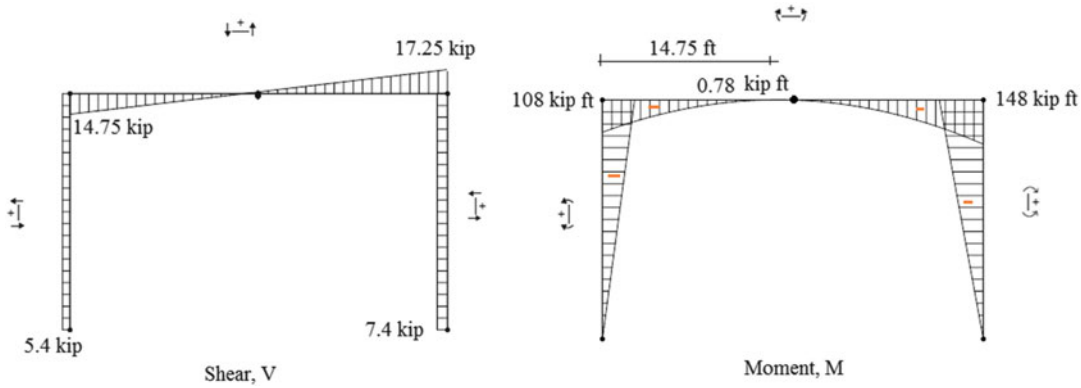

Fig. E4.5g Shear and moment diagrams

Example 4.6 Portal Frame with Overhang

Given: The portal frame defined in Fig. E4.6a.

Determine: The shear and moment diagrams.

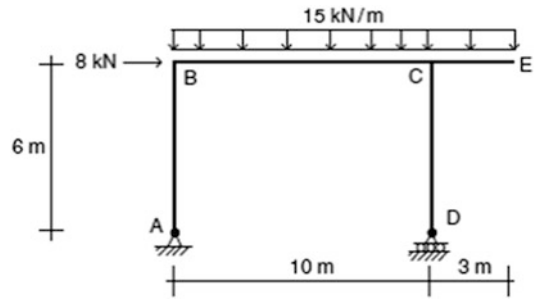

Fig. E4.6a

Solution: Results for the various analysis steps are listed in Figs. E4.6b, E4.6c, and E4.6d.

$$\sum M_{\mathrm{A}} = 0 \quad R_{\mathrm{D}}(10) - 8(6) - (15)(13)(6.5) = 0 \quad R_{\mathrm{D}} = 131.55\,\mathrm{kN} \uparrow$$
$$\sum F_x = 0 \quad R_{\mathrm{A}x} = 8\,\mathrm{kN} \leftarrow$$
$$\sum F_y = 0 \quad R_{\mathrm{A}y} + 131.55 - (15)(13) = 0 \quad R_{\mathrm{A}y} = 63.45\,\mathrm{kN} \uparrow$$

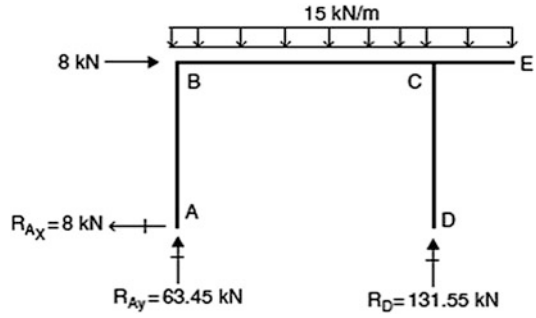

Fig. E4.6b Reactions

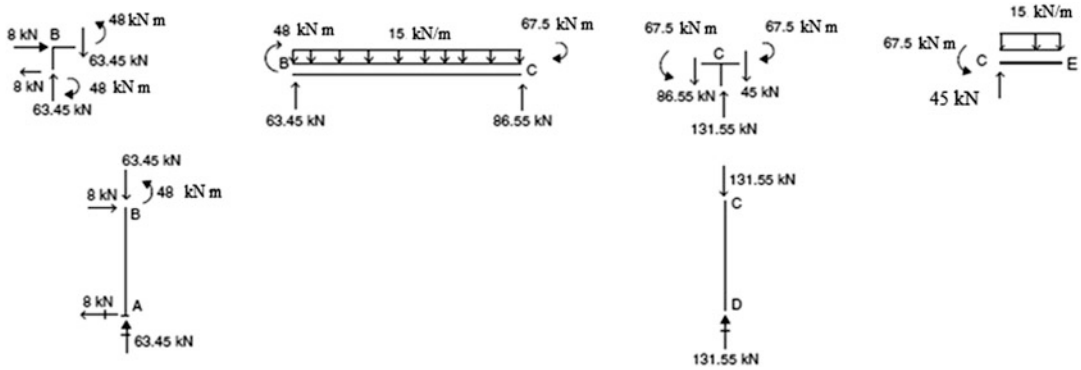

Fig. E4.6c End actions

First, we locate the maximum moment in member BC.

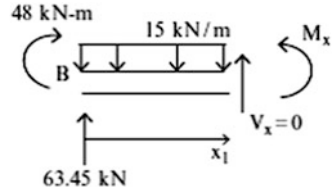

$$63.45 - (15)x_1 = 0 \rightarrow x_1 = 4.23\,\mathrm{m}$$

Then, $M_{\max} = 63.45(4.23) - \dfrac{(15)(4.23)^2}{2} + 48 = 182\,\mathrm{kN\,m}$

The corresponding shear and moment diagrams are listed in Fig. E4.6d.

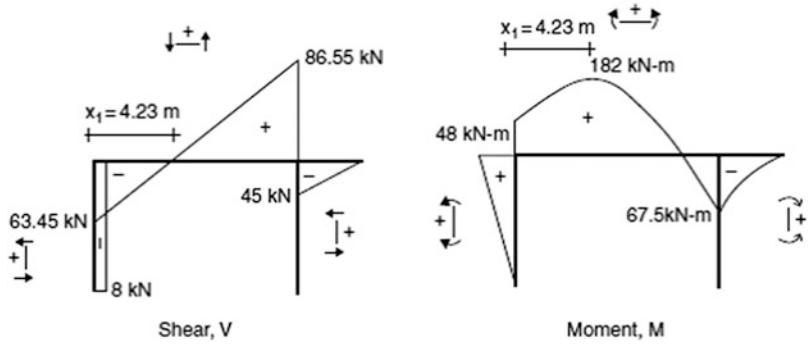

Fig. E4.6d Shear and moment diagrams

4.3.1 Behavior of Portal Frames: Analytical Solution

The previous examples illustrated numerical aspects of the analysis process for single-story statically determinate portal frames. For future reference, we list below the corresponding analytical solutions (Figs. 4.11, 4.12, 4.13, and 4.14). We consider both gravity and lateral loading. These solutions are useful for reasoning about the behavior of this type of frame when the geometric parameters are varied.

Portal frame—Gravity loading: Shown in Fig. 4.11
Portal frame—Lateral loading: Shown in Fig. 4.12
3-hinge portal frame—gravity loading: Shown in Fig. 4.13
3-hinge portal frame—lateral loading: Shown in Fig. 4.14

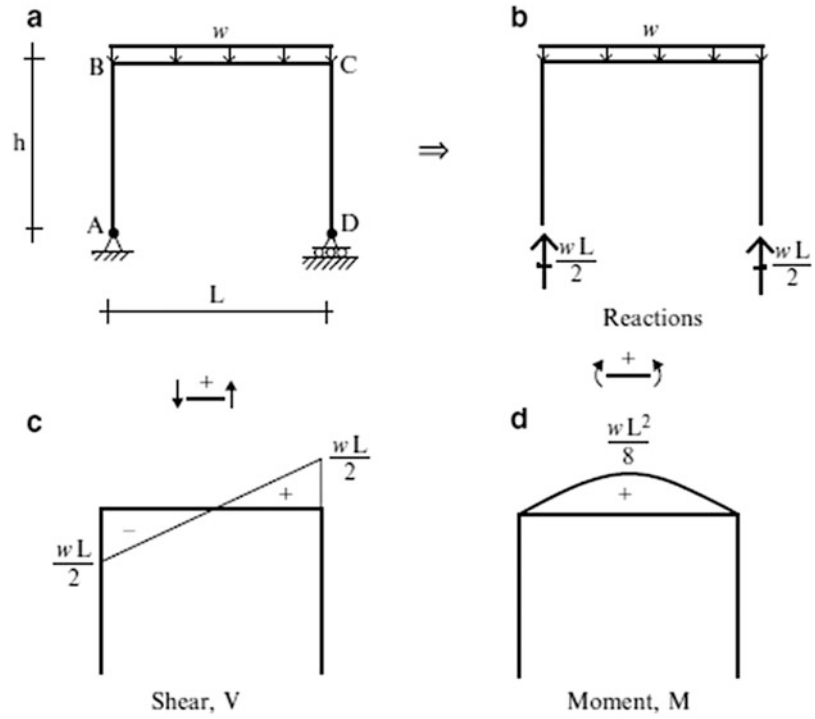

Fig. 4.11 Statically determinate portal frame under gravity loading. (**a**) Geometry and loading. (**b**) Reactions. (**c**) Shear diagram. (**d**) Moment diagram

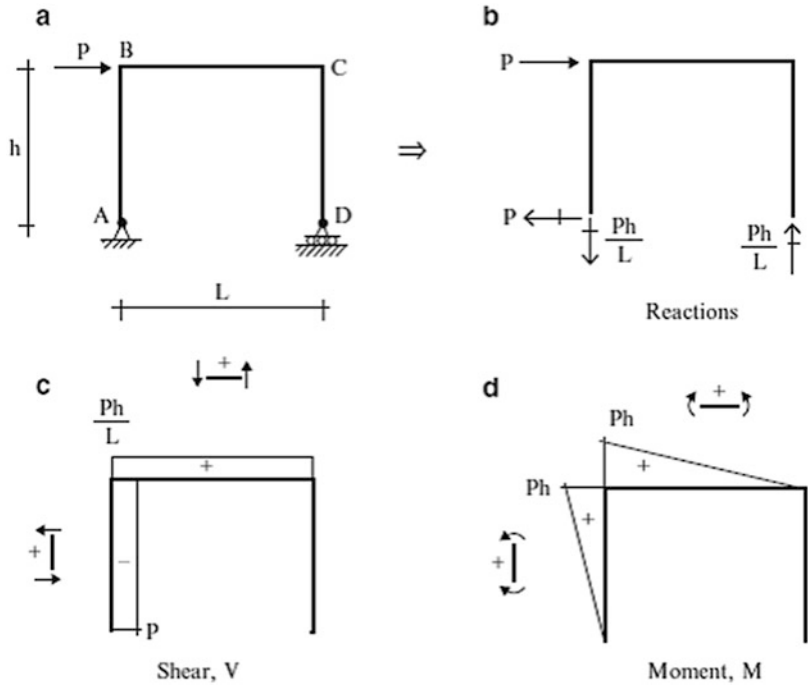

Fig. 4.12 Statically determinate portal frame under lateral loading. (**a**) Geometry and loading. (**b**) Reactions. (**c**) Shear diagram. (**d**) Moment diagram

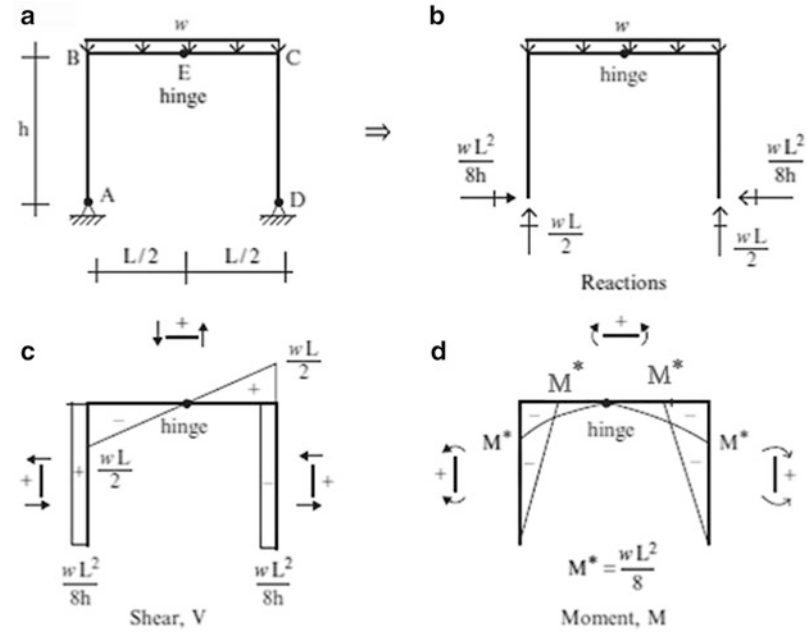

Fig. 4.13 Statically determinate 3-hinge portal frame under gravity loading. (**a**) Geometry and loading. (**b**) Reactions. (**c**) Shear diagram. (**d**) Moment diagram

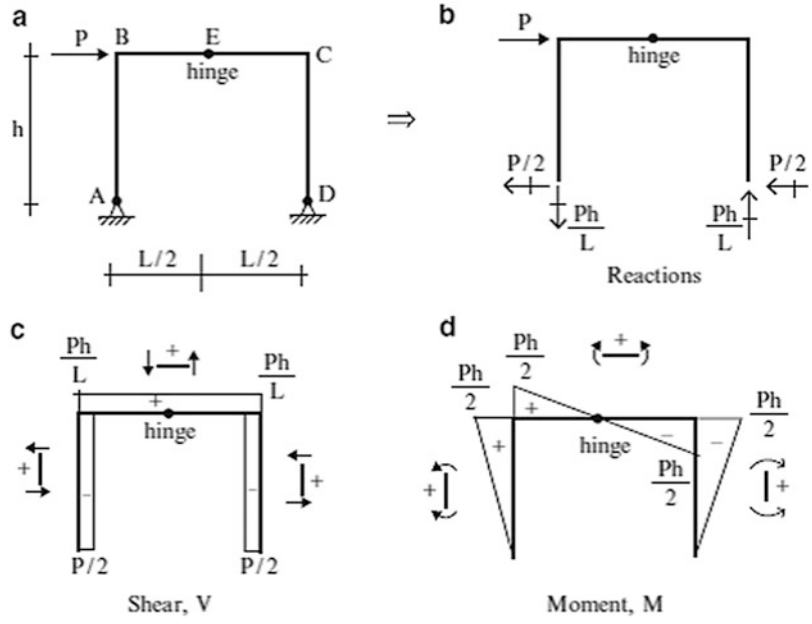

Fig. 4.14 Statically determinate 3-hinge portal frame under lateral loading. (**a**) Geometry and loading. (**b**) Reactions. (**c**) Shear diagram. (**d**) Moment diagram

Fig. 4.15 Variable cross-section 3-hinge frame

These results show that the magnitude of the peak moment due to the uniform gravity load is the *same* for both structures but of opposite sense (Figs. 4.11 and 4.13). The peak moment occurs at the corner points for the 3-hinge frame and at mid-span for the simply supported frame which behaves as a simply supported beam. The response under lateral loading is quite different (Figs. 4.12 and 4.14). There is a 50 % *reduction* in peak moment for the 3-hinge case due to the inclusion of an additional horizontal restraint at support D.

For the 3-hinge frame, we note that the bending moment diagram due to gravity loading is symmetrical. In general, a symmetrical structure responds symmetrically when the loading is symmetrical. We also note that the bending moment diagram for lateral loading applied to the 3-hinge frame is anti-symmetrical.

Both loadings produce moment distributions having peaks at the corner points. In strength-based design, the cross-sectional dimensions depend on the design moment; the deepest section is required by the peak moment. Applying this design approach to the 3-hinge frame, we can use variable depth members with the depth increased at the corner points and decreased at the supports and mid-span. Figure 4.15 illustrates a typical geometry. Variable depth 3-hinge frames are quite popular. We point out again here that the internal force distribution in statically determinate structures depends only on the loading and geometry and is independent of the cross-sectional properties of the members. Therefore, provided we keep the same geometry (centerline dimensions), we can vary the cross-section properties for a 3-hinge frame without changing the moment distributions.

4.4 Pitched Roof Frames

In this section, we deal with a different type of portal frame structure: the roof members are sloped upward to create a pitched roof. This design creates a more open interior space and avoids the problem of rain water pounding or snow accumulating on flat roofs. Figure 4.16 shows the structures under consideration. The first structure is a rigid frame with a combination of pin and roller supports; the second structure is a 3-hinge frame. Both structures are analyzed by first finding the reactions and then isolating individual members to determine the member end forces, and the internal force distributions.

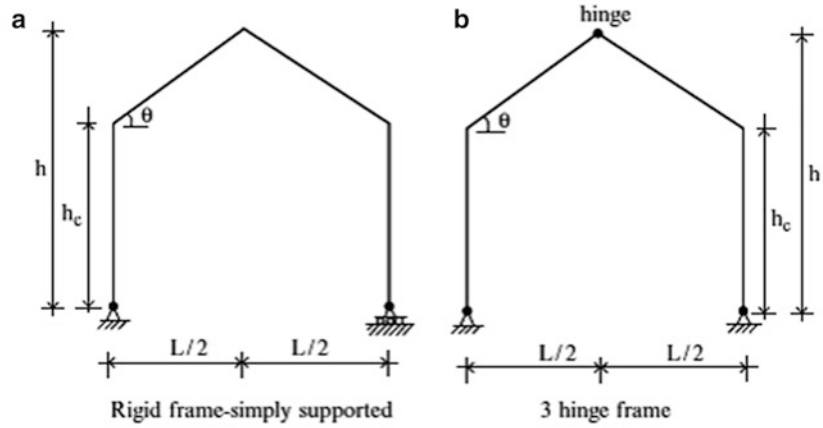

Fig. 4.16 Pitched roof frames

4.4.1 Member Loads

Typical loads that may be applied to an inclined member are illustrated in Fig. 4.17. They may act either in the vertical direction or normal to the member. In the vertical direction, they may be defined either in terms of the horizontal projection of the length of the member or in terms of the length of the member.

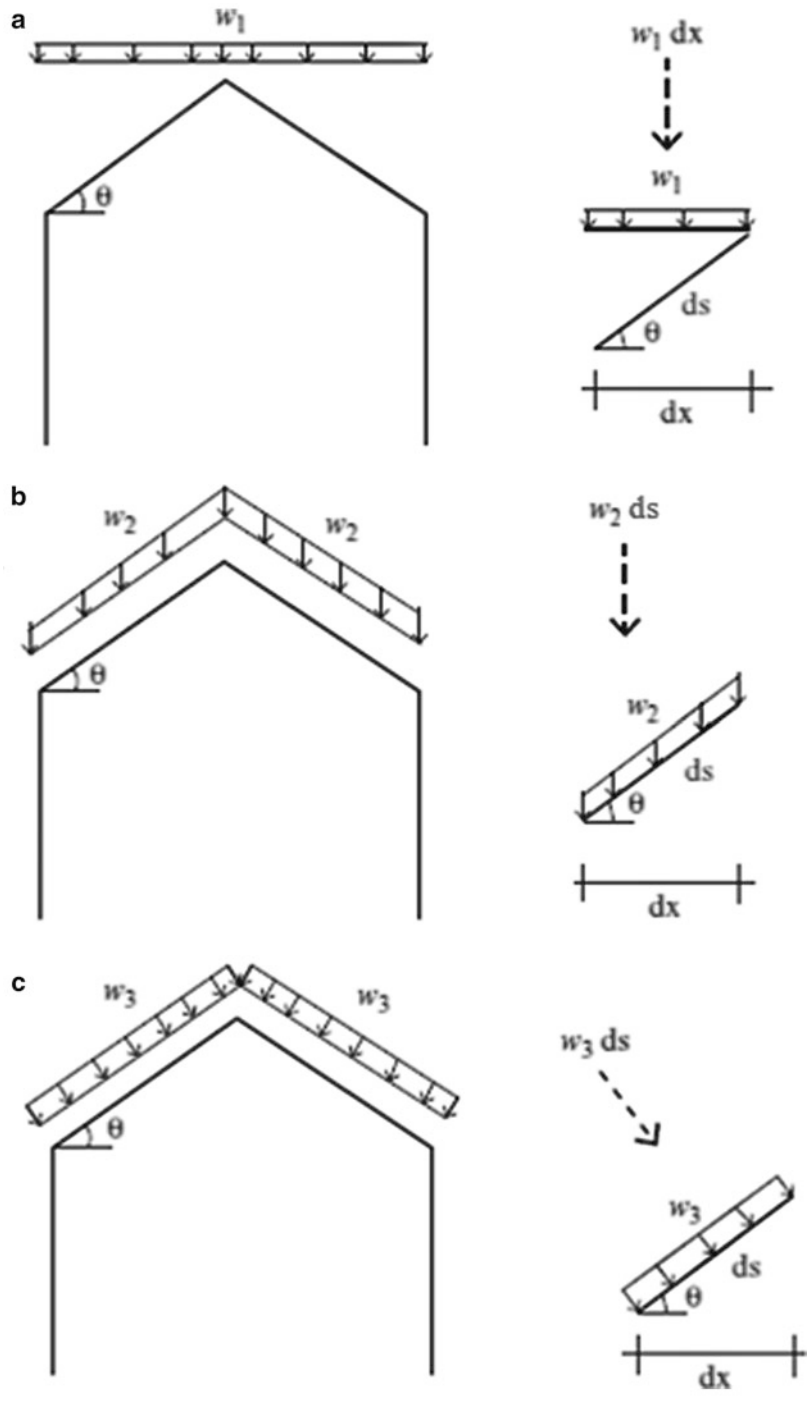

Fig. 4.17 Loading on an inclined member. (**a**) Vertical load per horizontal projection. (**b**) Vertical load per length. (**c**) Normal load per length

When computing the reactions, it is convenient to work with loads referred to horizontal and vertical directions and expressed in terms of the horizontal projection. The w_1 loading is already in this form. For the w_2 load, we note that

$$\mathrm{d}x = \mathrm{d}s \cos\theta$$

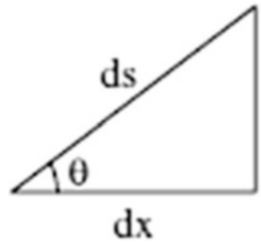

Then,

$$\begin{aligned} w_2 \mathrm{d}s &= \frac{w_2 \mathrm{d}x}{\cos\theta} \\ w_{2,\mathrm{v}} &= \frac{w_2}{\cos\theta} \end{aligned} \tag{4.3}$$

The w_3 load is normal to the member. We project it onto the vertical and horizontal directions and then substitute for ds.

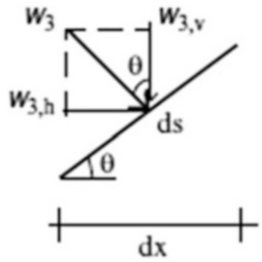

$$(w_3 \, \mathrm{d}s) \cos\theta = w_{3,\mathrm{v}} \, \mathrm{d}x$$

$$w_3 \, \mathrm{d}s \sin\theta = w_{3,\mathrm{h}} \, \mathrm{d}x$$

$$w_3 \frac{\mathrm{d}x}{\cos\theta} \sin\theta = w_{3,\mathrm{h}} \, \mathrm{d}x$$

The final result is

$$\begin{aligned} w_{3,\mathrm{v}} &= w_3 \\ w_{3,\mathrm{h}} &= w_3 \tan\theta \end{aligned} \tag{4.4}$$

It follows that the equivalent vertical loading per horizontal projection is equal to the normal load per unit length. These results are summarized in Fig. 4.18.

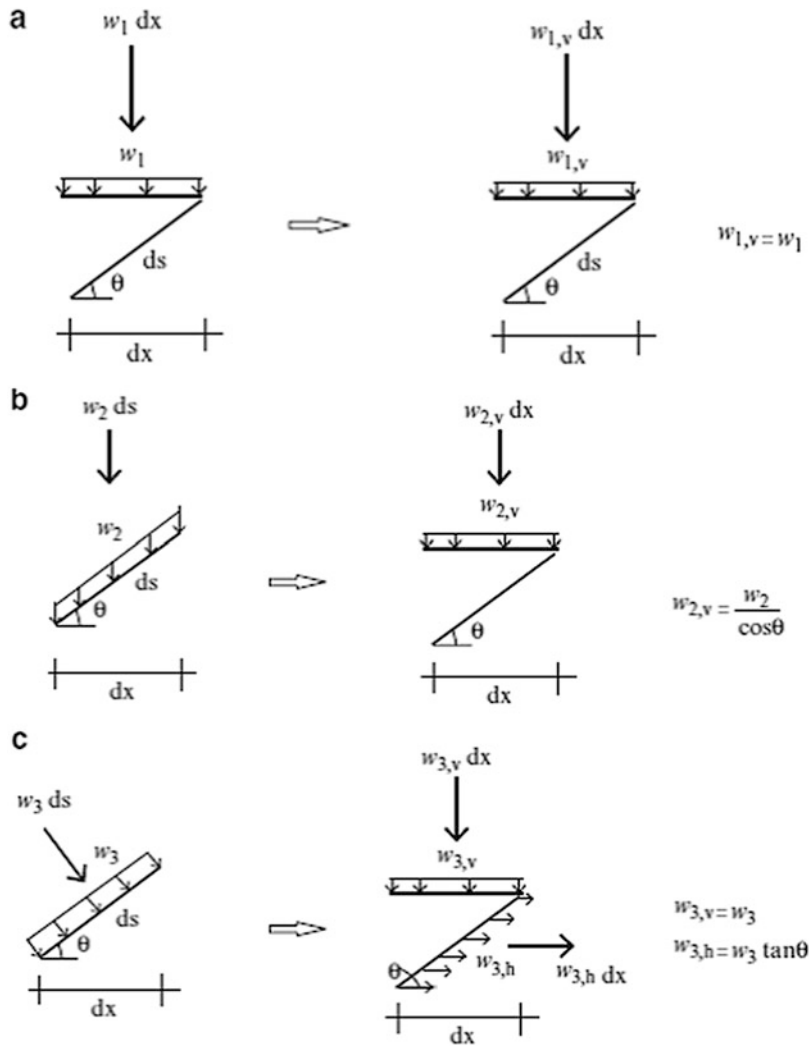

Fig. 4.18 Equivalent vertical member loadings. (**a**) Per horizontal projection. (**b**) Per length. (**c**) Normal load

When computing the axial force, shear, and moment distribution along a member, it is more convenient to work with loads referred to the normal and tangential directions of the member and expressed in terms of the member arc length. The approach is similar to the strategy followed above. The results, as summarized, below are (Fig. 4.19):

Vertical–horizontal projection loading:

$$\begin{aligned} w_{1,\mathrm{n}} &= w_1 \cos\theta^2 \\ w_{1,\mathrm{t}} &= w_1 \cos\theta \sin\theta \end{aligned} \tag{4.5}$$

Member loading:

$$\begin{aligned} w_{2,\mathrm{n}} &= w_2 \cos\theta \\ w_{2,\mathrm{t}} &= w_2 \sin\theta \\ w_{3,\mathrm{n}} &= w_3 \\ w_{3,\mathrm{t}} &= 0 \end{aligned} \tag{4.6}$$

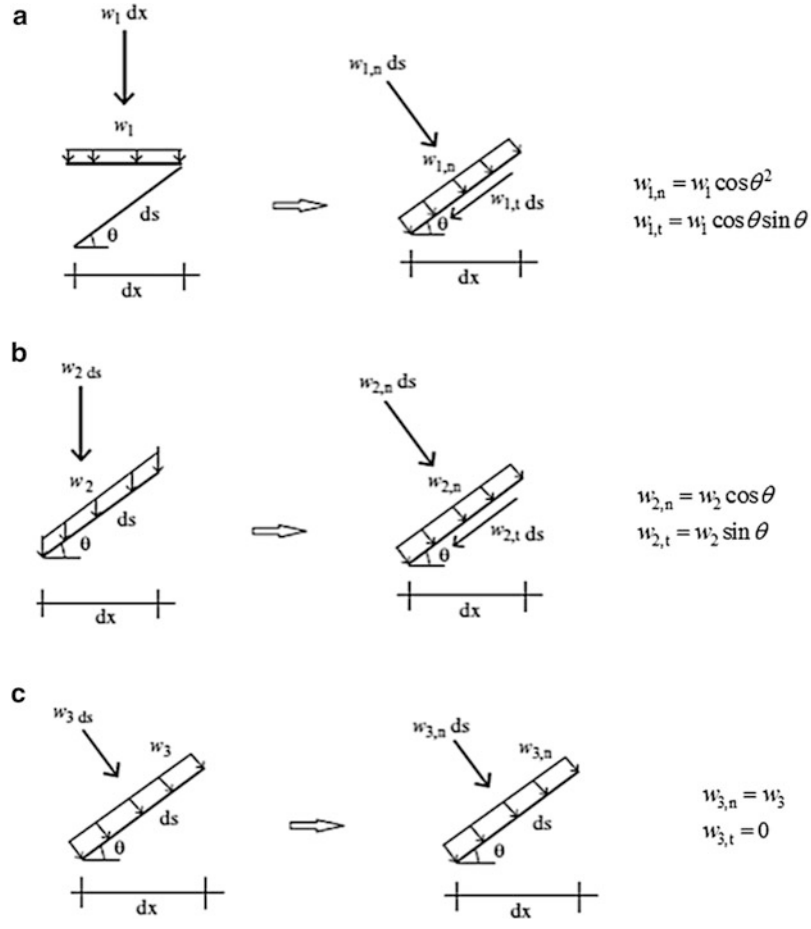

Fig. 4.19 Equivalent normal and tangential member loadings. (**a**) Vertical per projected length. (**b**) Vertical per length. (**c**) Normal

4.4.2 Analytical Solutions for Pitched Roof Frames

Analytical solutions for the bending moment distribution are tabulated in this section. They are used for assessing the sensitivity of the response to changes in the geometric parameters.

Gravity loading per unit horizontal projection: Results are listed in Figs. 4.20 and 4.21.

Lateral Loading: Results are listed in Figs. 4.22 and 4.23.

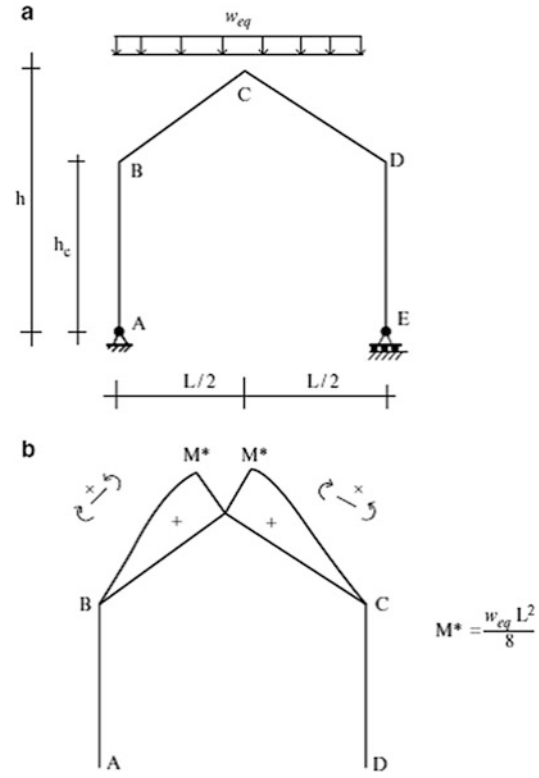

Fig. 4.20 Simply supported gable rigid frame. (**a**) Structure and loading. (**b**) Moment diagram

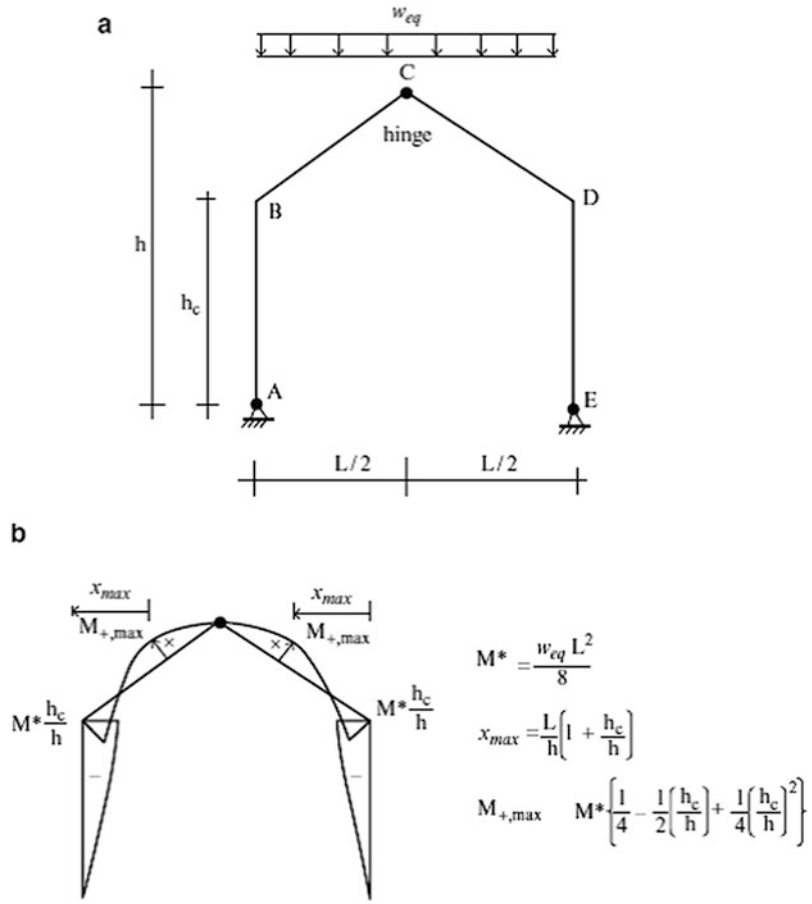

Fig. 4.21 3-Hinge frame under gravity loading. (**a**) Structure and loading. (**b**) Moment diagram

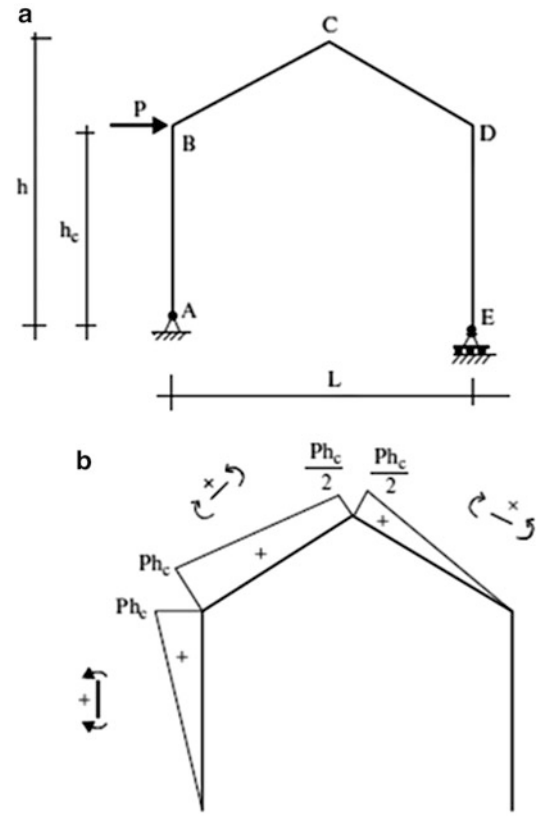

Fig. 4.22 Simply supported rigid frame—lateral loading. (**a**) Structure and loading. (**b**) Moment diagram

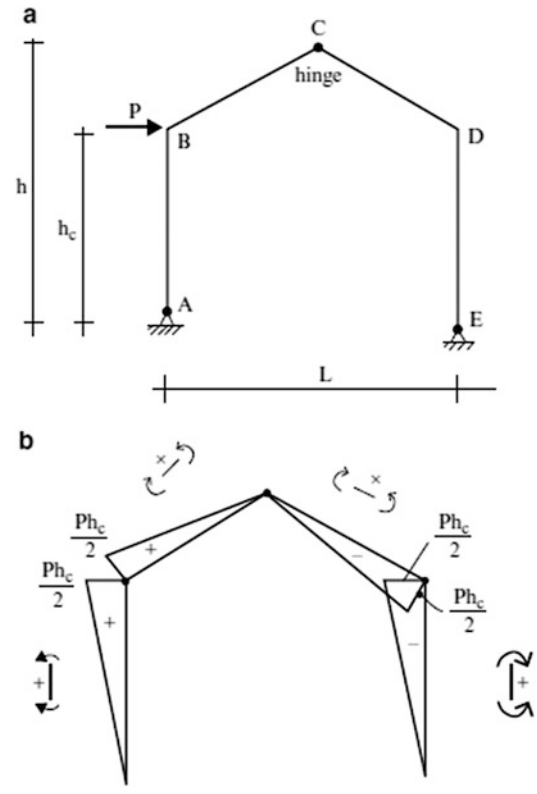

Fig. 4.23 3-Hinge frame—lateral loading. (**a**) Structure and loading. (**b**) Moment diagram

Example 4.7 Simply Supported Gable Frame—Lateral Load

Given: The gable frame with the lateral load defined in Fig. E4.7a.
Determine: The shear, moment, and axial force diagrams.

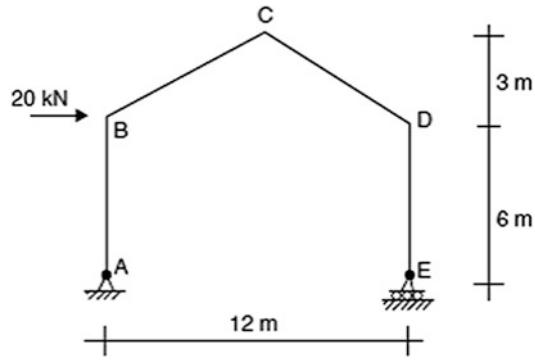

Fig. E4.7a

Solution: Moment summation about A leads to the vertical reaction at E. The reactions at A follow from force equilibrium considerations. Next, we determine the end forces and moments for the individual members. Lastly, we generate the shear and moment diagrams. Results for the various analysis steps are listed in Figs. E4.7b, E4.7c, E4.7d, and E4.7e.

Step 1: Reactions

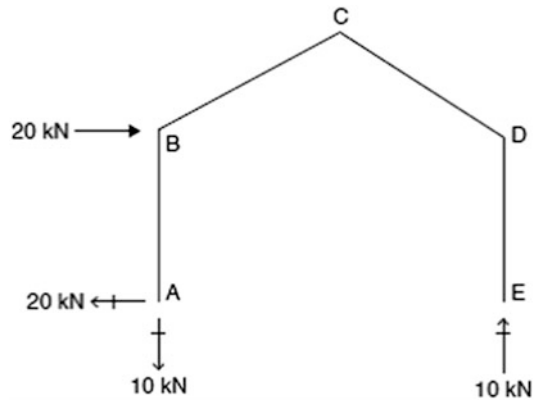

Fig. E4.7b Reactions

Step 2: End forces

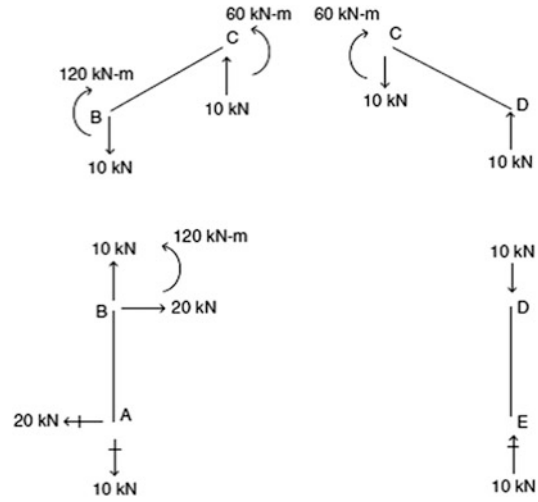

Fig. E4.7c End forces—global frame

Step 3: Member forces—member frames

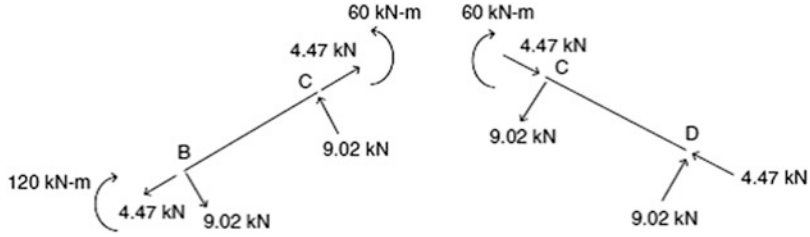

Fig. E4.7d End forces in local member frame

Step 4: Internal force diagrams

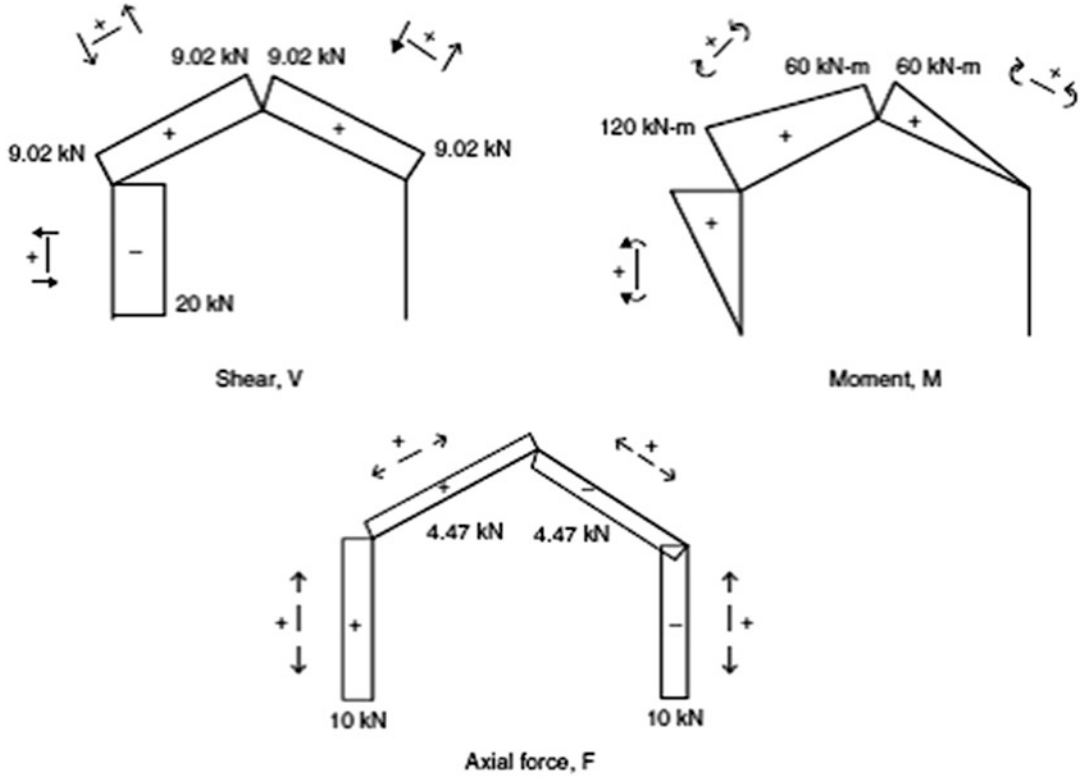

Fig. E4.7e Force distributions

Example 4.8 3-Hinge Gable Frame—Lateral Loading

Given: The 3-hinge gable frame shown in Fig. E4.8a.

Determine: The shear, moment, and axial force diagrams.

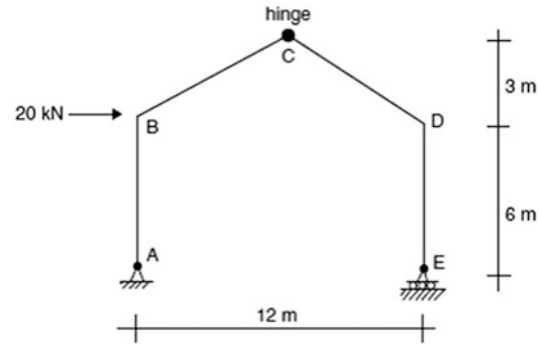

Fig. E4.8a

Solution:

Step 1: Reactions

The reactions (Fig. E4.8b) are determined by summing moments about A and C and applying the force equilibrium conditions.

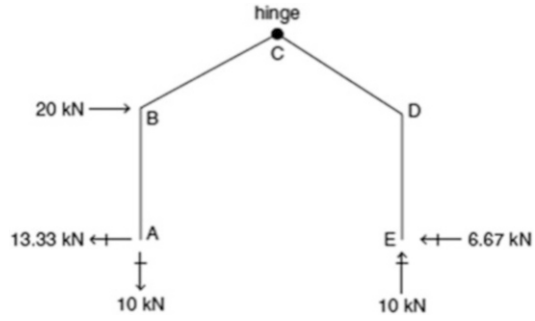

Fig. E4.8b Reactions

Step 2: End forces—global frame (Fig. E4.8c)

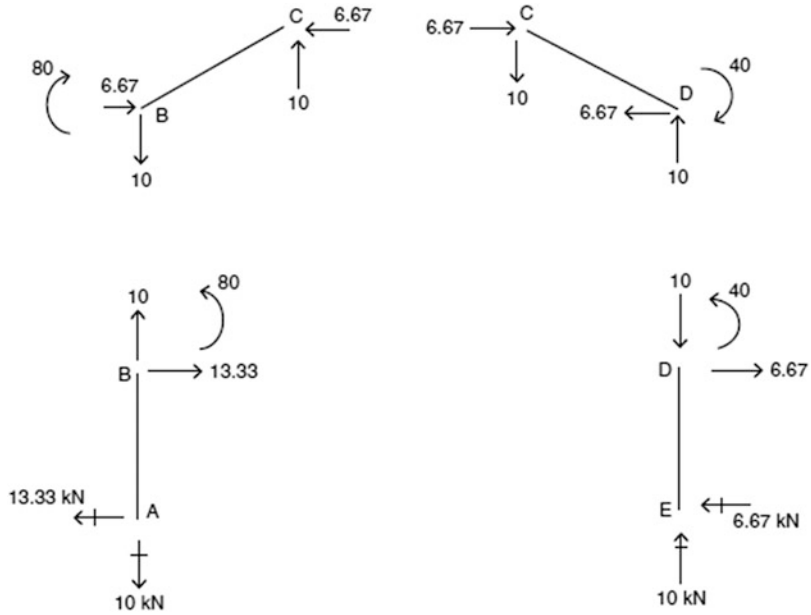

Fig. E4.8c End forces

Step 3: End forces—local member frame

Figure E4.8d shows the end forces and moments resolved into components referred to the local member frame.

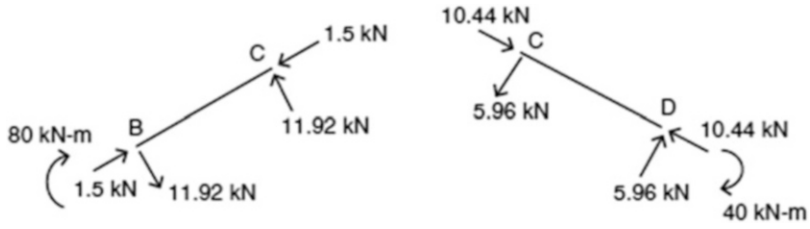

Fig. E4.8d End actions in local member frame

Step 4: Internal force distribution (Fig. E4.8e)

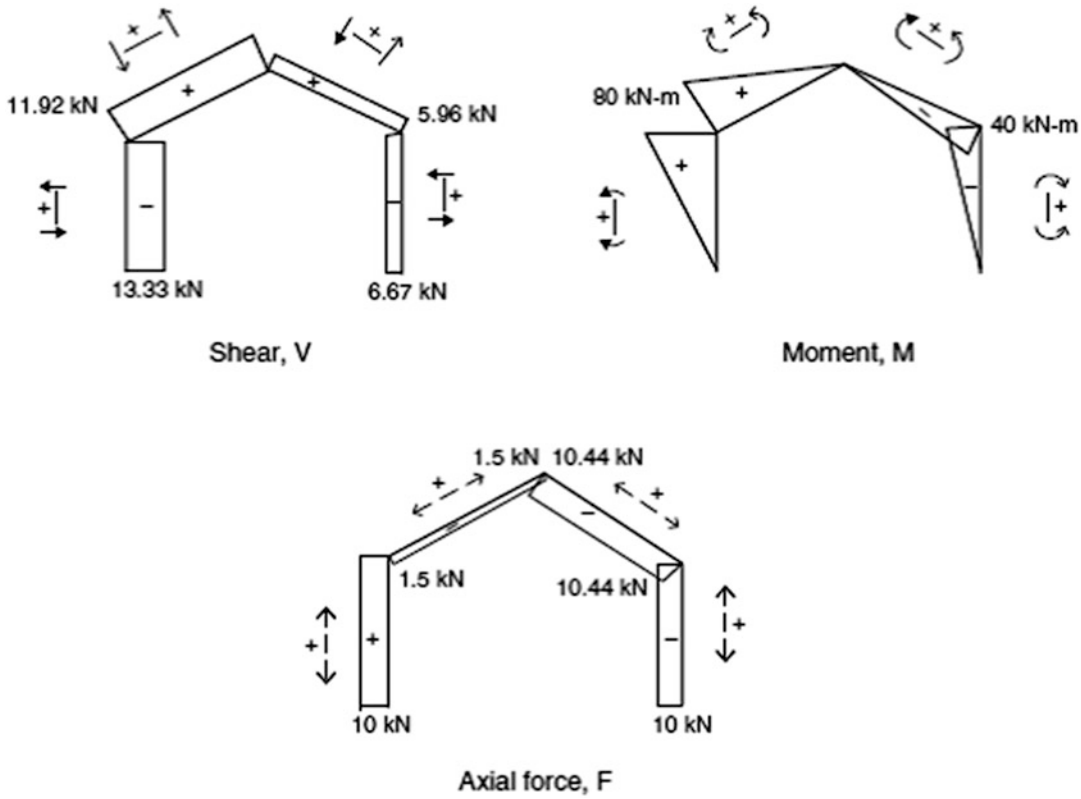

Fig. E4.8e Force distributions

Note that the 3-hinge gable structure has a lower value of peak moment.

Example 4.9 Simply Supported Gable Frame—Unsymmetrical Loading

Given: The frame defined in Fig. E4.9a. The loading consists of a vertical load per horizontal projection applied to member BC.

Determine: The member force diagrams.

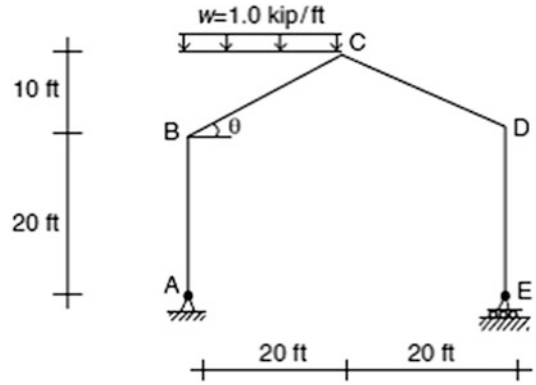

Fig. E4.9a

Solution: The reactions at E and A are determined by summing moments about A and by enforcing vertical equilibrium. Figure E4.9b shows the results.

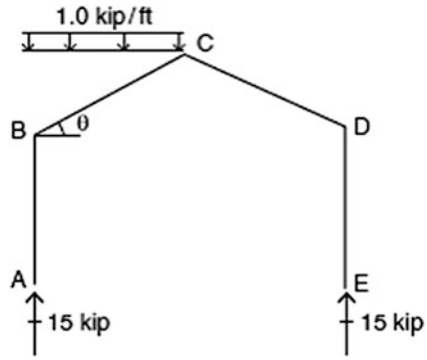

Fig. E4.9b Reactions

Next, we determine the end forces and moments for the individual members. Then, we need to resolve the loading and the end forces for members BC and CD into normal and tangential components. The transformed quantities are listed in Figs. E4.9c and E4.9d.

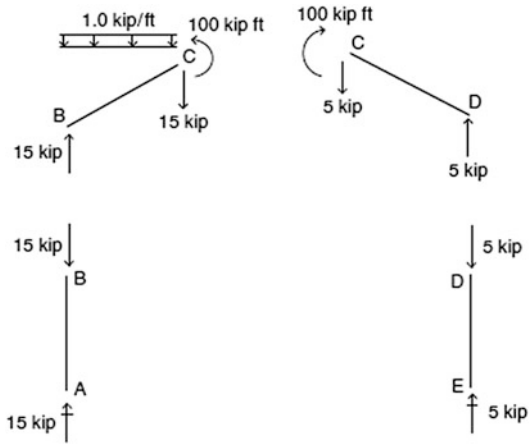

Fig. E4.9c End actions—global frame

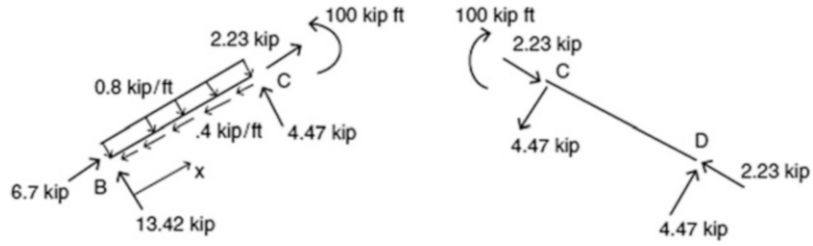

Fig. E4.9d End actions—local frame

The maximum moment in member BC occurs at x_1. We determine the location by setting the shear equal to zero.

$$13.42 - 0.8x_1 = 0 \Rightarrow x_1 = 16.775$$

Then, $M_{\max} = 13.42(16.775) - 0.8(16.775)^2\left(\frac{1}{2}\right) = 112.56\,\text{kip ft}$

Figure E4.9e contains the shear, moment, and axial force diagrams.

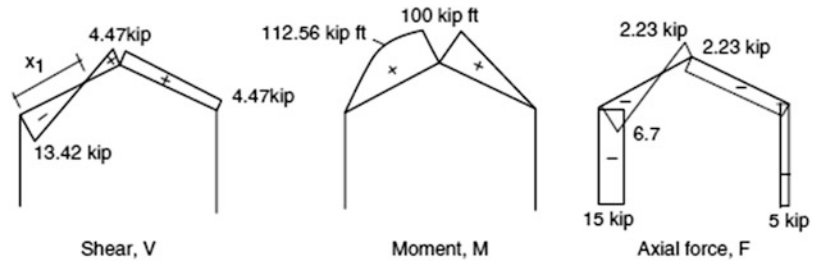

Fig. E4.9e Internal force diagrams

Example 4.10 3-Hinge Gable Frame

Given: The 3-hinge gable frame shown in Fig. E4.10a.

Determine: The shear and moment diagrams.

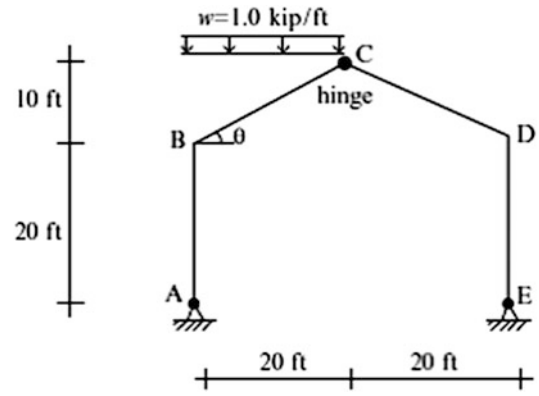

Fig. E4.10a

Solution: We analyzed a similar loading condition in Example 4.9. The results for the different analysis phases are listed in Figs. E4.10b, E4.10c, and E4.10d. Comparing Fig. E4.10e with Fig. E4.9e shows that there is a substantial *reduction* in the magnitude of the maximum moment when the 3-hinged gable frame is used.

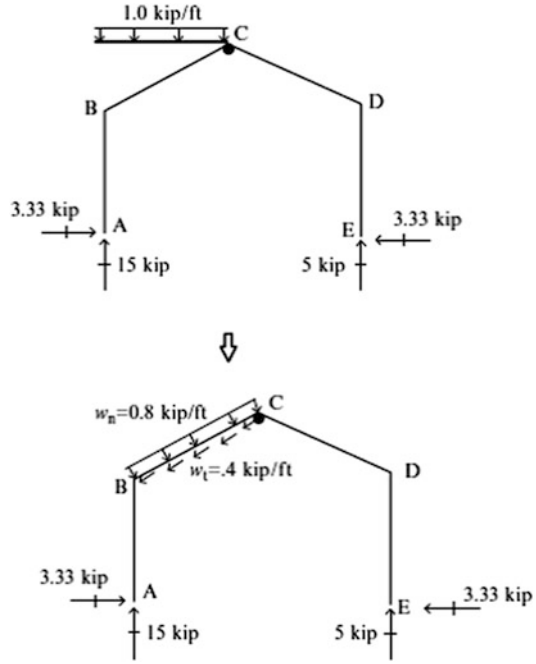

Fig. E4.10b Reactions

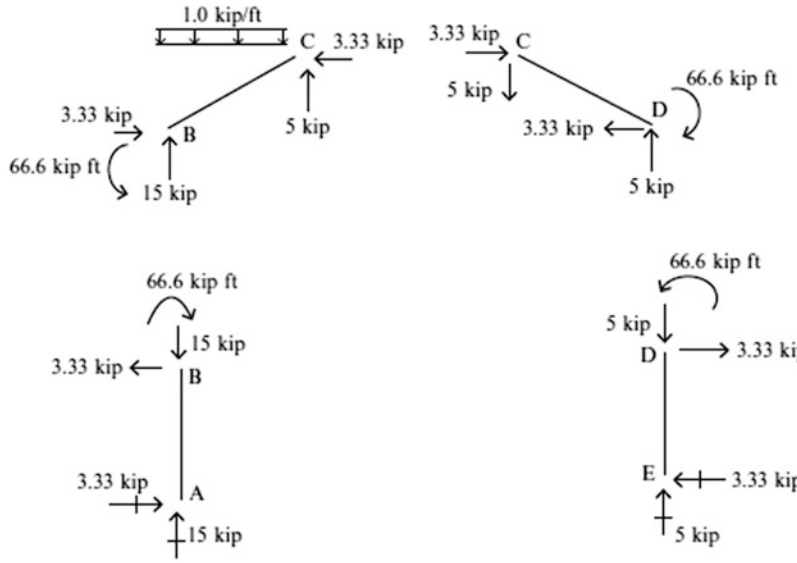

Fig. E4.10c End forces

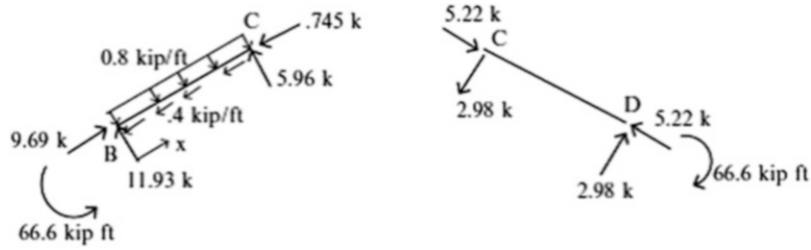

Fig. E4.10d End forces in local frame

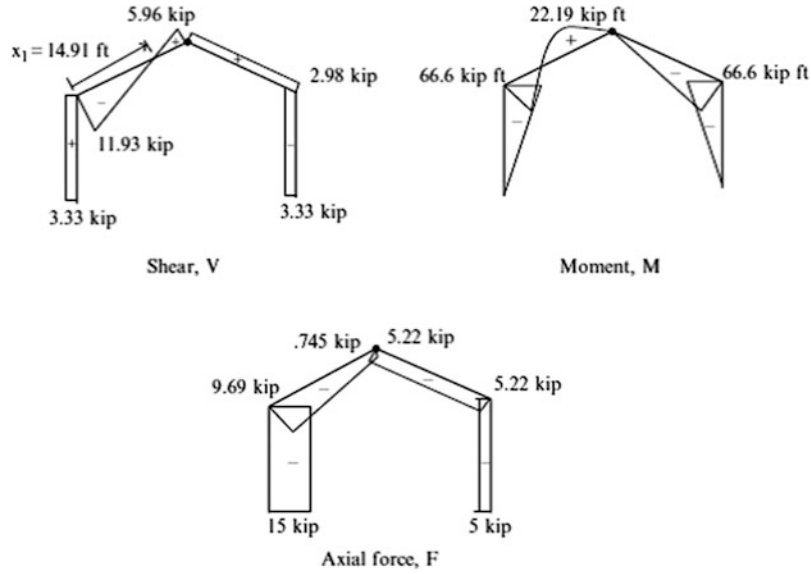

Fig. E4.10e Shear and moment diagrams

4.5 A-Frames

A-frames are obviously named for their geometry. Loads may be applied at the connection points or on the members. A-frames are typically supported at the base of their legs. Because of the nature of the loading and restraints, the members in an A-frame generally experience bending as well as axial force.

We consider first the triangular frame shown in Fig. 4.24. The inclined members are subjected to a uniform distributed loading per unit length w_g which represents the self-weight of the members and the weight of the roof that is supported by the member.

We convert w_g to an equivalent vertical loading per horizontal projection w using (4.3). We start the analysis process by first finding the reactions at A and C.

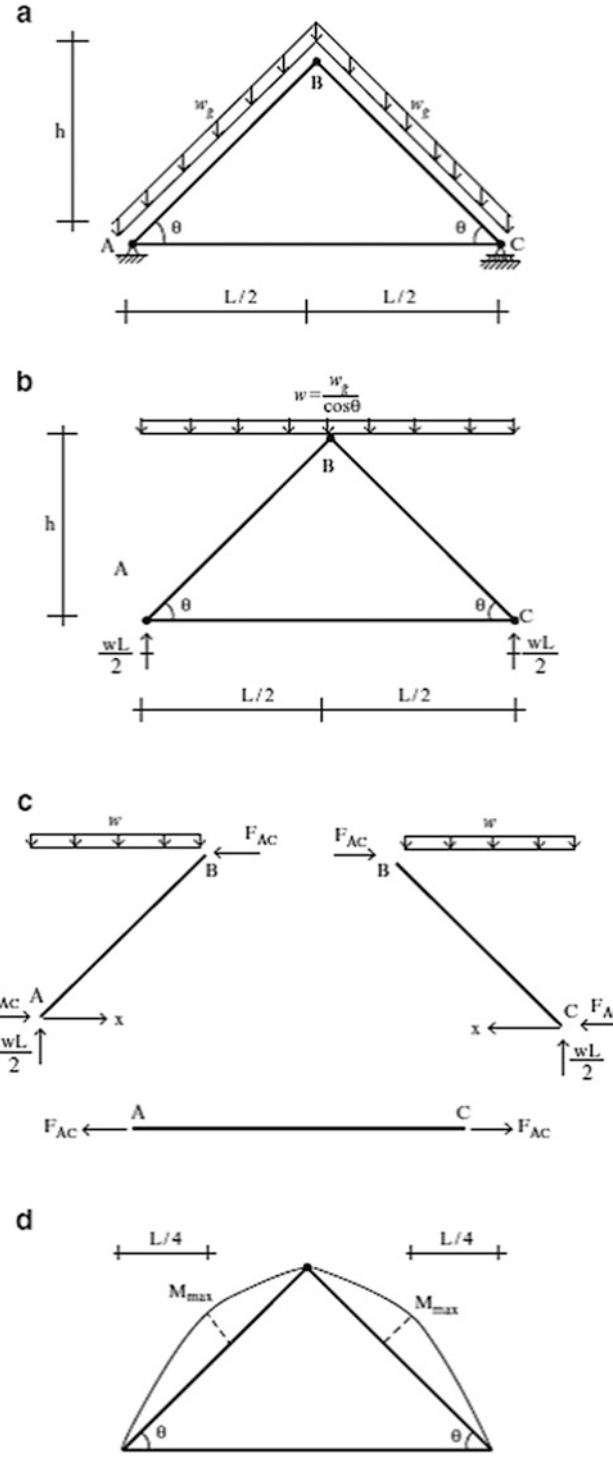

Fig. 4.24 (**a**) Geometry and loading. (**b**) A-frame loading and reactions. (**c**) Free body diagrams. (**d**) Moment diagram

Next, we isolate member BC (see Fig. 4.24c).

$$\sum M_{\text{at B}} = -\frac{w}{2}\left(\frac{L}{2}\right)^2 + \frac{wL}{2}\left(\frac{L}{2}\right) - hF_{\text{AC}} = 0$$

$$\Downarrow$$

$$F_{\text{AC}} = \frac{wL^2}{8h}$$

The horizontal internal force at B must equilibrate F_{AC}. Lastly, we determine the moment distribution in members AB and BC. Noting Fig. 4.24c, the bending moment at location x is given by

$$M(x) = \frac{wL}{2}x - F_{\text{AC}}\left(\frac{2h}{L}\right)x - \frac{wx^2}{2} = \frac{wL}{4}x - \frac{wx^2}{2}$$

The maximum moment occurs at $x = L/4$ and is equal to

$$M_{\max} = \frac{wL^2}{32}$$

Replacing w with w_{g}, we express $M_{\max}$ as

$$M_{\max} = \left(\frac{w_{\text{g}}}{\cos\theta}\right)\frac{L^2}{32}$$

As θ increases, the moment increases even though the projected length of the member remains constant.

We discuss next the frame shown in Fig. 4.25a. There are two loadings: a concentrated force at B and a uniform distributed loading applied to DE.

We first determine the reactions and then isolate member BC.

Summing moments about A leads to

$$P\left(\frac{L}{2}\right) + \frac{wL}{2}\left(\frac{L}{2}\right) = R_{\text{C}}L \quad R_{\text{C}} = \frac{P}{2} + \frac{wL}{4}$$

The results are listed below. Noting Fig. 4.25d, we sum moments about B to determine the horizontal component of the force in member DE.

$$\frac{L}{2}\left(\frac{P}{2} + \frac{wL}{4}\right) = \frac{wL}{4}\frac{L}{4} + \frac{h}{2}F_{\text{de}}$$

$$F_{\text{de}} = \frac{PL}{2h} + \frac{wL^2}{8h}$$

The bending moment distribution is plotted in Fig. 4.25e. Note that there is bending in the legs even though P is applied at node A. This is due to the location of member DE. If we move member DE down to the supports A and C, the moment in the legs would vanish.

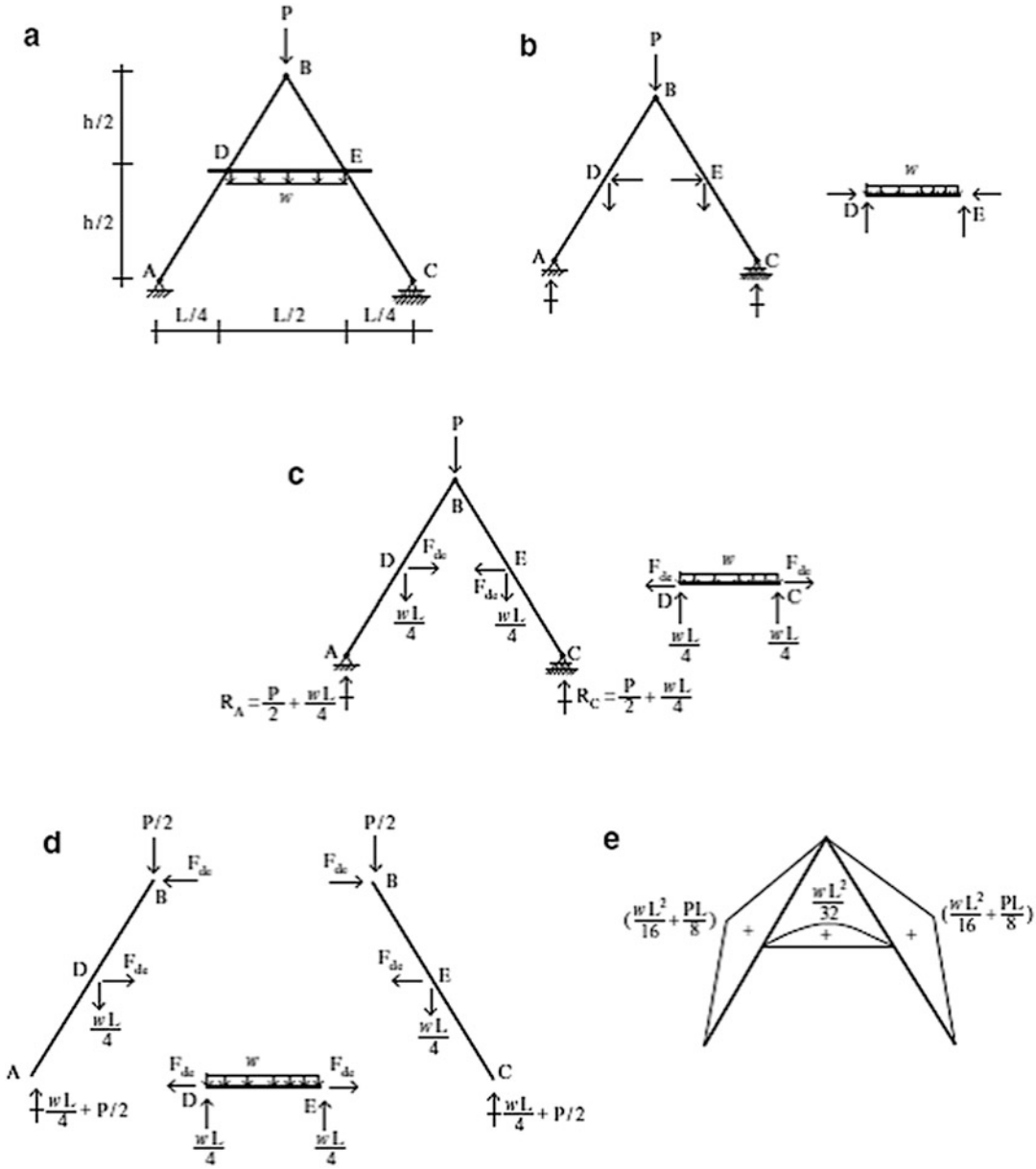

Fig. 4.25 (**a**) A-frame geometry and loading. (**b–d**) Free body diagrams. (**e**) Bending moment distribution

4.6 Deflection of Frames Using the Principle of Virtual Forces

The Principle of Virtual Forces specialized for a planar frame structure subjected to planar loading is derived in [1]. The general form is

$$d\,\delta P = \sum_{\text{members}} \int_s \left\{ \frac{M}{EI}\,\delta M + \frac{F}{AE}\delta F + \frac{V}{GA_s}\delta V \right\} \mathrm{d}s \tag{4.7}$$

Frames carry loading primarily by bending action. Axial and shear forces are developed as a result of the bending action, but the contribution to the displacement produced by shear deformation is generally small in comparison to the displacement associated with bending deformation and axial deformation. Therefore, we neglect this term and work with a reduced form of the principle of Virtual Forces.

$$d\,\delta P = \sum_{\text{members}} \int_s \left\{ \frac{M}{EI}\,\delta M + \frac{F}{AE}\delta F \right\} \mathrm{d}s \tag{4.8}$$

where δP is either a unit force (for displacement) or a unit moment (for rotation) in the direction of the desired displacement d; δM, and δF are the virtual moment and axial force due to δP. The integration is carried out over the length of each member and then summed up.

For low-rise frames, i.e., where the ratio of height to width is on the order of unity, the axial deformation term is also small. In this case, one neglects the axial deformation term in (4.8) and works with the following form

$$d\,\delta P = \sum_{\text{members}} \int_s \left(\frac{M}{EI} \right) (\delta M) \mathrm{d}s \tag{4.9}$$

Axial deformation is significant for tall buildings, and (4.8) is used for this case. In what follows, we illustrate the application of the Principle of Virtual Forces to some typical low-rise structures. We revisit this topic later in Chap. 9, which deals with statically indeterminate frames.

Example 4.11 Computation of Deflections—Cantilever-Type Structure

Given: The structure shown in Fig. E4.11a. Assume EI is constant.

$$E = 29,000\,\text{ksi}, \quad I = 300\,\text{in.}^4$$

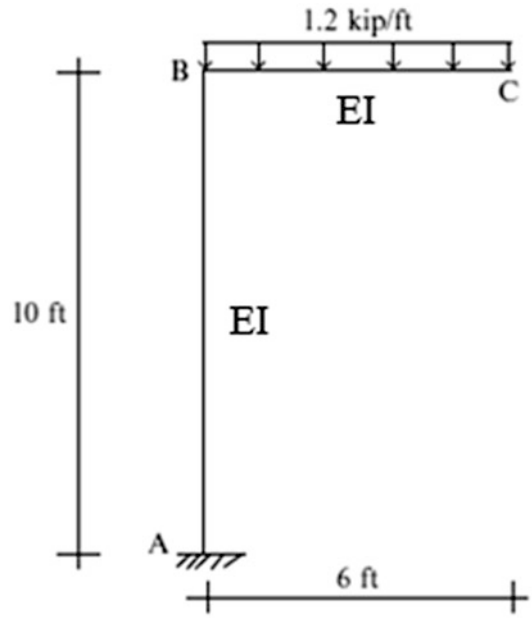

Fig. E4.11a

Determine: The horizontal and vertical deflections and the rotation at point C, the tip of the cantilever segment.

Solution: We start by evaluating the moment distribution corresponding to the applied loading. This is defined in Fig. E4.11b. The virtual moment distributions corresponding to u_c, v_c, and θ_c are defined in Figs. E4.11c, E4.11d, and E4.11e, respectively. Note that we take δP to be either a unit force (for displacement) or a unit moment (for rotation).

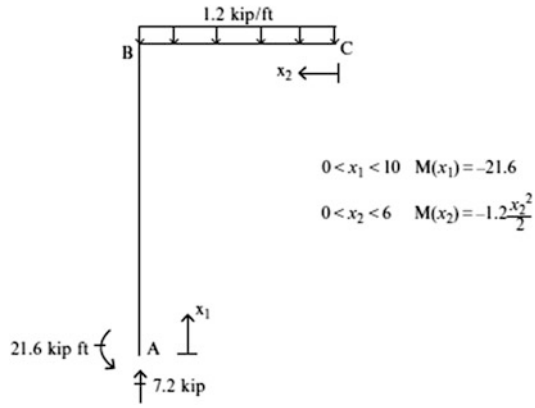

Fig. E4.11b $M(x)$

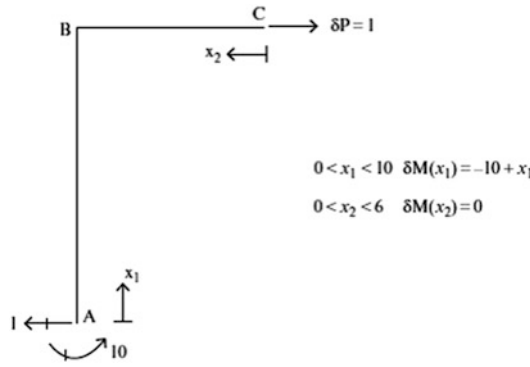

Fig. E4.11c $\delta M(x)$ for u_c

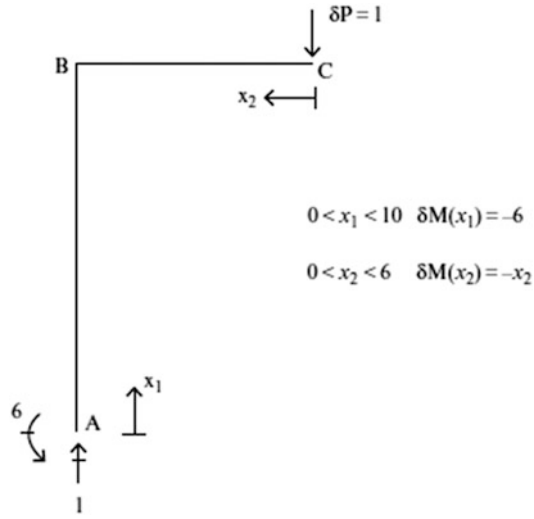

Fig. E4.11d $\delta M(x)$ for v_c

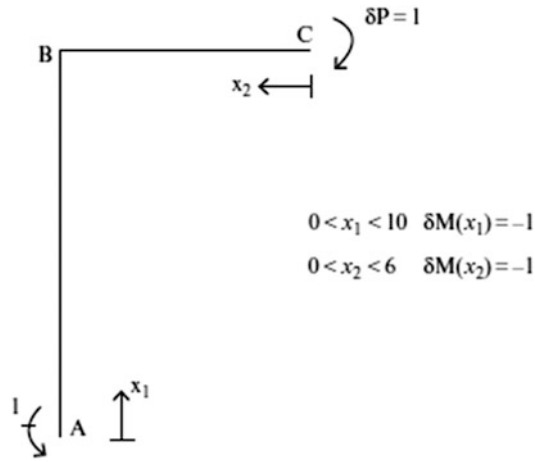

Fig. E4.11e $\delta M(x)$ for θ_c

We divide up the structure into two segments AB and CB and integrate over each segment. The total integral is given by

$$\sum_{\text{members}} \int_s \left(\frac{M}{EI}\delta M\right) \mathrm{d}s = \int_{\text{AB}} \left(\frac{M}{EI}\delta M\right) \mathrm{d}x_1 + \int_{\text{CB}} \left(\frac{M}{EI}\delta M\right) \mathrm{d}x_2$$

The expressions for u_c, v_c, and θ_c are generated using the moment distributions listed above.

$$EIu_C = \int_0^{10} (-21.6)(-10 + x_1)\mathrm{d}x_1 = 1080\,\text{kip ft}^3$$

$$u_C = \frac{1080(12)^3}{29,000(300)} = 0.2145\,\text{in.} \rightarrow$$

$$EIv_C = \int_0^{10} (-21.6)(-6)\mathrm{d}x_1 + \int_0^6 \left(-\frac{1.2}{2}x_2^2\right)(-x_2)\mathrm{d}x_2 = 1490\,\text{kip ft}^3$$

$$v_C = \frac{1490(12)^3}{29,000(300)} = 0.296\,\text{in.} \downarrow$$

$$EI\theta_C = \int_0^{10} (-21.6)(-1)\mathrm{d}x_1 + \int_0^6 \left(-\frac{1.2}{2}x_2^2\right)(-1)\mathrm{d}x_2 = 259\,\text{kip ft}^2$$

$$\theta_C = \frac{259(12)^2}{29,000(300)} = 0.0043\,\text{rad clockwise}$$

Example 4.12 Computation of Deflections

Given: The structure shown in Fig. E4.12a. $E = 29{,}000$ ksi, $I = 900$ in.^{4}

Determine: The horizontal displacements at points C and D and the rotation at B.

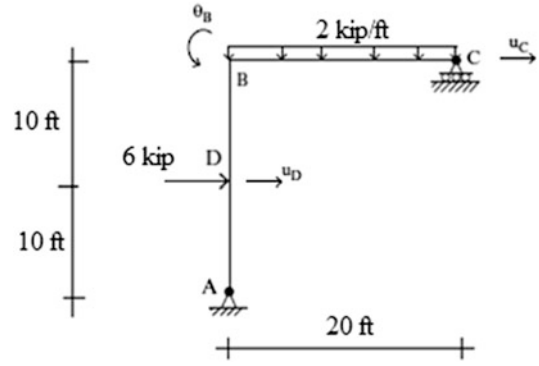

Fig. E4.12a

Solution: We start by evaluating the moment distribution corresponding to the applied loading. This is defined in Fig. E4.12b.

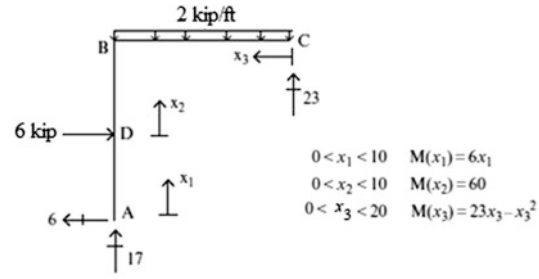

Fig. E4.12b $M(x)$

The virtual moment distributions corresponding to u_c and u_D are listed in Figs. E4.12c and E4.12d.

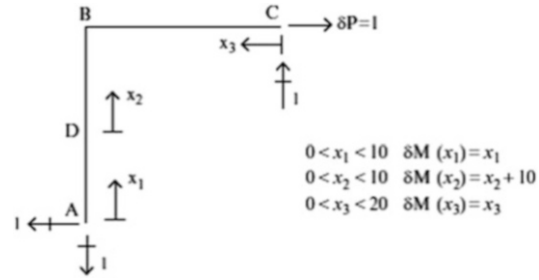

Fig. E4.12c δM for u_C

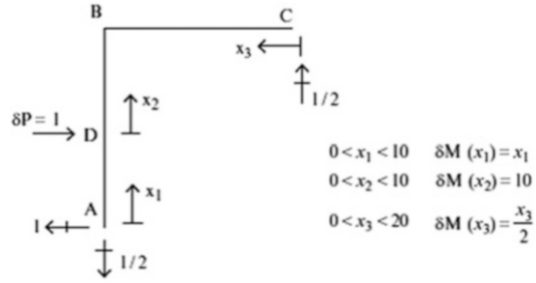

Fig. E4.12d δM for u_D

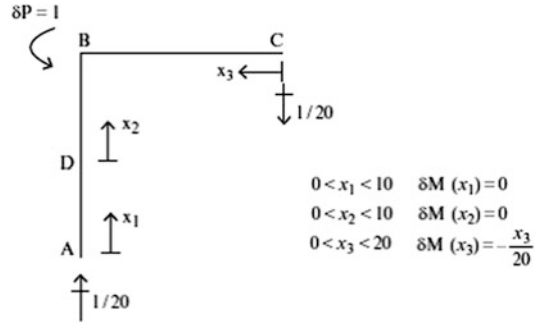

Fig. E4.12e δM for θ_B

We express the total integral as the sum of three integrals.

$$\sum_{\text{members}} \int_s \left(\frac{M}{EI}\,\delta M\right) \mathrm{d}s = \int_{\text{AD}} \left(\frac{M}{EI}\,\delta M\right) \mathrm{d}x_1 + \int_{\text{DB}} \left(\frac{M}{EI}\,\delta M\right) \mathrm{d}x_2 + \int_{\text{CB}} \left(\frac{M}{EI}\,\delta M\right) \mathrm{d}x_3$$

The corresponding form for u_c is

$$EIu_C = \int_0^{10} 6x_1(x_1)\mathrm{d}x_1 + \int_0^{10} (x_2 + 10)(60)\mathrm{d}x_2 + \int_0^{20} \left(23x_3 - x_3^2\right)(x_3)$$

$$\mathrm{d}x_3 = \left|2x_1^3\right|_0^{10} + \left|30x_2^2 + 600x_2\right|_0^{10} + \left|\frac{23x_3^3}{3} - \frac{x_3^4}{4}\right|_0^{20} = 32,333\,\text{kip ft}^3$$

$$u_C = \frac{32,333 \times (12)^3}{(29,000)(900)} = 2.14\,\text{in.} \rightarrow$$

Following a similar procedure, we determine u_D

$$EIu_D = \int_0^{10} 6x_1(x_1)dx_1 + \int_0^{10} 60(10)dx_2 + \int_0^{20} (23x_3 - x_3^2)\left(\frac{x_2}{3}\right)dx_3$$

$$= \left|2x_1^3\right|_0^{10} + |600x_2|_0^{10} + \left|\frac{23x_3^3}{6} - \frac{1}{8}x_3^4\right|_0^{20} = 18,667\,\text{kip ft}^3$$

$$u_D = \frac{18,667(12)^3}{(29,000)(900)} = 1.23\,\text{in.} \rightarrow$$

Lastly, we determine θ_B (Fig. E4.12e)

$$EI\theta_B = \int_0^{20} (23x_3 - x_3^2)\left(-\frac{x_3}{20}\right)dx_3$$

$$= \left|-\frac{23x_3^3}{60} + \frac{x_3^4}{80}\right|_0^{20} = -106,667\,\text{kip ft}^2$$

$$\theta_B = -\frac{106,667(12)^2}{(29,000)(900)} = -0.0059$$

The minus sign indicates the sense of the rotation is opposite to the initial assumed sense.

$$\theta_B = 0.0059\,\text{rad clockwise}$$

Example 4.13 Computation of Deflection

Given: The steel structure shown in Figs. E4.13a, E4.13b, and E4.13c. Take $I_b = \frac{4}{3}I_c$, $h_C = 4\,\text{m}$, $L_b = 3\,\text{m}$, $P = 40\,\text{kN}$, and $E = 200\,\text{GPa}$.

Determine: The value of I_C required to limit the horizontal displacement at C to be equal to 40 mm.

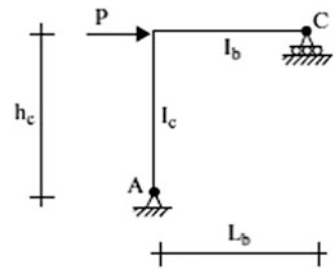

Fig. E4.13a

Solution: We divide up the structure into two segments and express the moments in terms of the local coordinates x_1 and x_2.

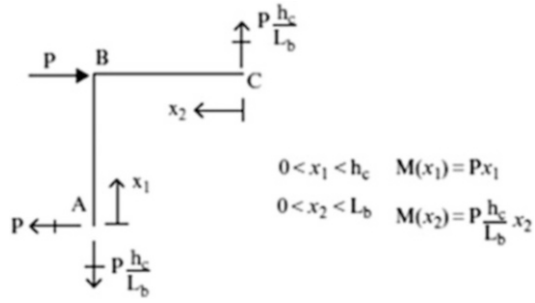

Fig. E4.13b $M(x)$

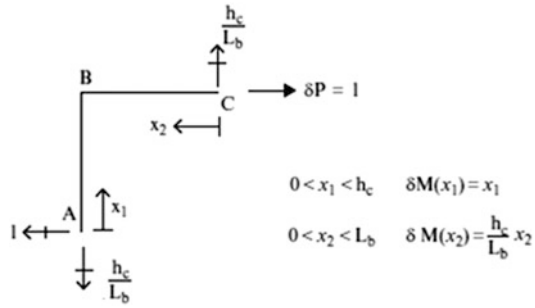

Fig. E4.13c δM for u_C

We express the total integral as the sum of two integrals.

$$\sum_{\text{members}} \int_s \left(\frac{M}{EI}\delta M\right) \mathrm{d}s = \int_{\mathrm{AB}} \left(\frac{M}{EI}\delta M\right) \mathrm{d}x_1 + \int_{\mathrm{CB}} \left(\frac{M}{EI}\delta M\right) \mathrm{d}x_2$$

The corresponding expression for u_C is

$$u_C = \frac{1}{EI_c}\int_0^{h_c} (Px_1)(x_1)\mathrm{d}x_1 + \frac{1}{EI_b}\int_0^{L_b} \left(P\frac{h_c}{L_b}x_2\right)\left(\frac{h_c}{L_b}x_2\right)\mathrm{d}x_2$$

$$\Downarrow$$

$$u_C = \frac{P}{EI_c}\int_0^{h_c} (x_1)^2\mathrm{d}x_1 + \frac{P}{EI_b}\left(\frac{h_c}{L_b}\right)^2 \int_0^{L_b} (x_2)^2\mathrm{d}x_2$$

$$\Downarrow$$

$$u_C = \frac{Ph_c^3}{3EI_c} + \frac{PL_b^3}{3EI_b}\left(\frac{h_c}{L_b}\right)^2 = \frac{Ph_c^2}{3E}\left(\frac{h_c}{I_c} + \frac{L_b}{I_b}\right)$$

Then, for $I_b = \frac{4}{3}I_c$, the I_C required is determined with

$$u_C = \frac{Ph_c^2}{3E}\left(\frac{h_c}{I_c} + \frac{L_b}{I_b}\right) = \frac{40(4000)^2}{3(200)}\left(\frac{4000}{I_c} + \frac{3000}{(4/3)I_c}\right) = 40$$

$$\therefore I_c = 167(10)^6 \text{mm}^4$$

Example 4.14 Computation of Deflection—Non-prismatic Member

Given: The non-prismatic concrete frame shown in Figs. E4.14a and E4.14b.

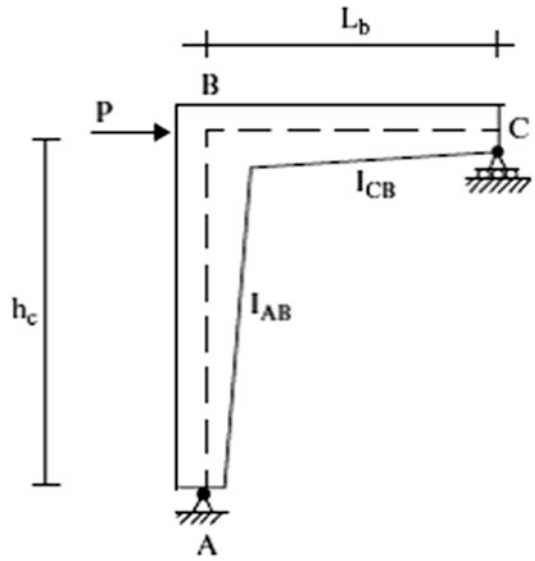

Fig. E4.14a Non-prismatic frame

Assume $h_C = 12\,\text{ft}, L_b = 10\,\text{ft}, P = 10\,\text{kip}$, and $E = 4000\,\text{ksi}$. Consider the member depths (d) to vary linearly and the member widths (b) to be constant. Assume the following geometric ratios:

$$d_{AB,1} = 2\,d_{AB,0}$$

$$d_{CB,1} = 1.5\,d_{CB,0}$$

$$b = \frac{d_{AB,0}}{2}$$

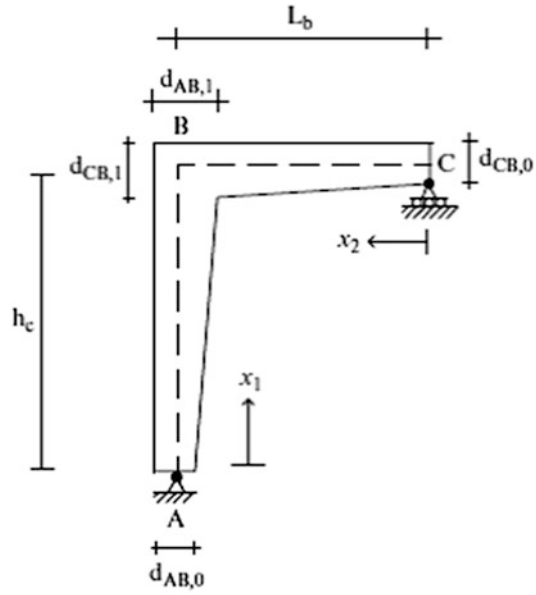

Fig. E4.14b Cross section depths

Determine:

(a) A general expression for the horizontal displacement at C (u_C).
(b) Use numerical integration to evaluate u_C as a function of $d_{AB,0}$.
(c) The value of $d_{AB,0}$ for which $u_C = 1.86$ in.

Solution:

Part (a): The member depth varies linearly. For member AB,

$$d(x_1) = d_{AB,0}\left(1 - \frac{x_1}{h_c}\right) + d_{AB,1}\left(\frac{x_1}{h_c}\right) = d_{AB,0}\left\{1 + \frac{x_1}{h_c}\left(\frac{d_{AB,1}}{d_{AB,0}} - 1\right)\right\}$$
$$= d_{AB,0}\, g_{AB}\left(\frac{x_1}{h_c}\right)$$

Then,

$$I_{AB} = I_{AB,0}(g_{AB})^3$$

Similarly, for member BC

$$d(x_2) = d_{CB,0}\left\{1 + \frac{x_2}{L_b}\left(\frac{d_{CB,1}}{d_{CB,0}} - 1\right)\right\} = d_{CB,0}\, g_{CB}\left(\frac{x_2}{L_b}\right)$$
$$I_{CB} = I_{CB,0}(g_{CB})^3$$

We express the moments in terms of the local coordinates x_1 and x_2.

$$M(x_1) = Px_1 \qquad 0 < x_1 < h_c$$

$$M(x_2) = P\frac{h_c}{L_b}x_2 \qquad 0 < x_2 < L_b$$

$$\delta M(x_1) = x_1 \qquad 0 < x_1 < h_c$$

$$\delta M(x_2) = \frac{h_c}{L_b}x_2 \qquad 0 < x_2 < L_b$$

The moment distributions are listed below.

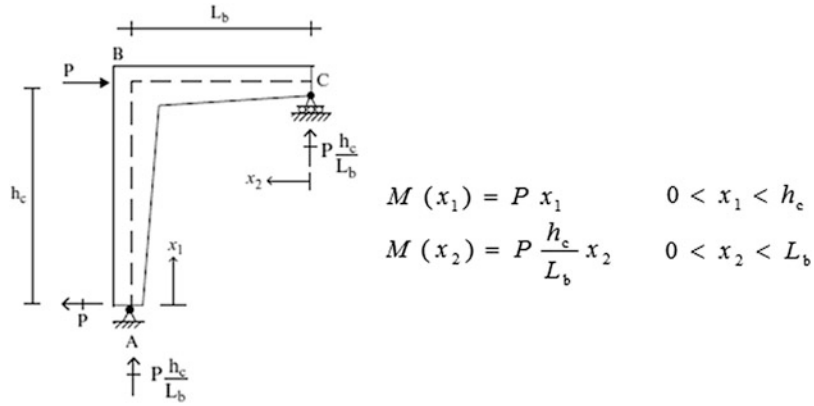

Fig. E4.14c $M(x)$

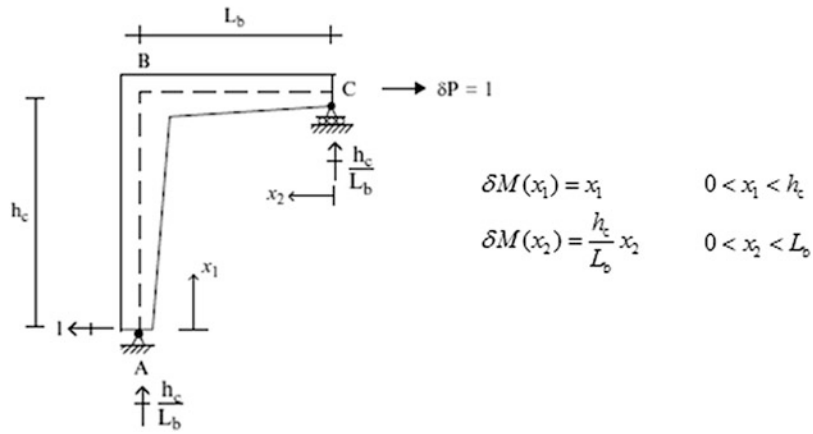

Fig. E4.14d δM for u_C

$$u_C = \frac{1}{E}\int_0^{h_c}\frac{1}{I_{AB}}(Px_1)(x_1)\mathrm{d}x_1 + \frac{1}{E}\int_0^{L_b}\frac{1}{I_{CB}}\left(P\frac{h_c}{L_b}x_2\right)\left(\frac{h_c}{L_b}x_2\right)\mathrm{d}x_2$$

Substituting for I_{AB} and I_{CB} and expressing the integral in terms of the dimensionless values $x_1/h = \overline{x}_1$ and $x_2/L_b = \overline{x}_2$, the expression for u_C reduces to

$$u_C = \frac{P(h_c)^3}{EI_{AB,0}} \int_0^1 \frac{(\bar{x}_1^2)\mathrm{d}\bar{x}_1}{(g_{AB})^3} + \frac{P(h_c/L_b)^2(L_b)^3}{EI_{CB,0}} \int_0^1 \frac{(\bar{x}_2^2)\mathrm{d}\bar{x}_2}{(g_{CB})^3}$$

Taking $g_{AB} = g_{CB} = 1$ leads to the values for the integrals obtained in Example 3.13, i.e., 1/3.

Part (b): Using the specified sections, the g functions take the form

$$g_{AB} = 1 + \frac{x_1}{h} = 1 + \bar{x}_1$$

$$g_{CB} = 1 + \frac{1x_2}{2L_b} = 1 + \frac{1}{2}\bar{x}_2$$

Then, the problem reduces to evaluating the following integrals:

$$J_1 = \int_0^1 \frac{(\bar{x}_1^2)\mathrm{d}\bar{x}_1}{(1+\bar{x}_1)^3} \quad \text{and} \quad J_2 = \int_0^1 \frac{(\bar{x}_2^2)\mathrm{d}\bar{x}_2}{(1+(1/2)\bar{x}_2)^3}$$

We compute these values using the trapezoidal rule. Results for different interval sizes are listed below.

N	J_1	J_2
10	0.0682	0.1329
20	0.0682	0.1329
25	0.0682	0.1329
30	0.0682	0.1329

Next, we specify the inertia terms

$$I_{AB,0} = \frac{b(d_{AB,0})^3}{12}$$

$$I_{BC,0} = \frac{b(d_{CB,0})^3}{12}$$

For $I_{AB,0} = (3/4)I_{CB,0}$, the expression for u_C reduces to

$$u_C = \frac{P}{EI_{AB,0}} \left\{ h_c^3 J_1 + \left(\frac{h_c}{L_b}\right)^2 (L_b)^3 \left(\frac{3}{4}\right)(J_2) \right\}$$

Part(c): Setting $u_C = 1.86$ and solving for $I_{AB,0}$ leads to

$$I_{AB,0} = \frac{P}{Eu_C} \left\{ h_c^3 J_1 + \left(\frac{h_c}{L_b}\right)^2 (L_b)^3 \left(\frac{3}{4}\right)(J_2) \right\} = 607\,\text{in.}^2$$

Finally,

$$d_{AB,0} = \{24 I_{AB,0}\}^{1/4} = 10.98\,\text{in.}$$

$$d_{CB,0} = \left\{\tfrac{4}{3}\right\}^{1/3} \quad d_{AB,0} = 12.1\,\text{in.}$$

4.7 Deflection Profiles: Plane Frame Structures

Applying the principle of Virtual Forces leads to specific displacement measures. If one is more interested in the overall displacement response, then it is necessary to generate the displacement profile for the frame. We dealt with a similar problem in Chap. 3, where we showed how to sketch the deflected shapes of beams given the bending moment distributions. We follow essentially the same approach in this section. Once the bending moment is known, one can determine the curvature, as shown in Fig. 4.26.

In order to establish the deflection profile for the entire frame, one needs to construct the profile for each member, and then join up the individual shapes such as that the displacement restraints are satisfied. We followed a similar strategy for planar beam-type structures; however, the process is somewhat more involved for plane frames.

Consider the portal frame shown in Fig. 4.27. Bending does not occur in AB and CD since the moment is zero. Therefore, these members must remain straight. However, BC bends into a concave shape. The profile consistent with these constraints is plotted below. Note that B, C, and D move laterally under the vertical loading.

Suppose we convert the structure into the 3-hinge frame defined in (Fig. 4.28). Now, the moment diagram is negative for all members. In this case, the profile is symmetrical. There is a discontinuity in the slope at E because of the moment release.

Fig. 4.26 Moment-curvature relationship

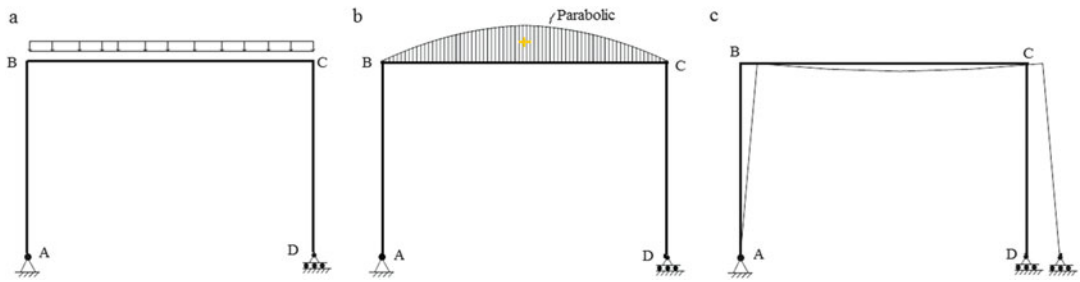

Fig. 4.27 Portal frame. (**a**) Loading. (**b**) Bending moment. (**c**) Deflection profile

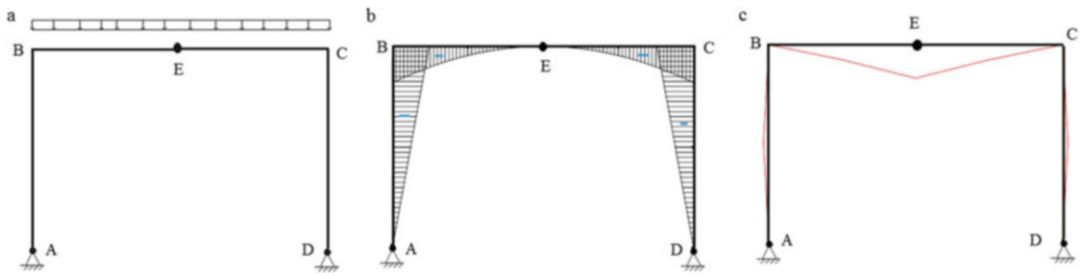

Fig. 4.28 3-Hinge frame. (**a**) Loading. (**b**) Bending moment. (**c**) Deflection profile

Gable frames are treated in a similar manner. The deflection profiles for simply supported and 3-hinge gable frames acted upon by gravity loading are plotted below (Figs. 4.29 and 4.30).

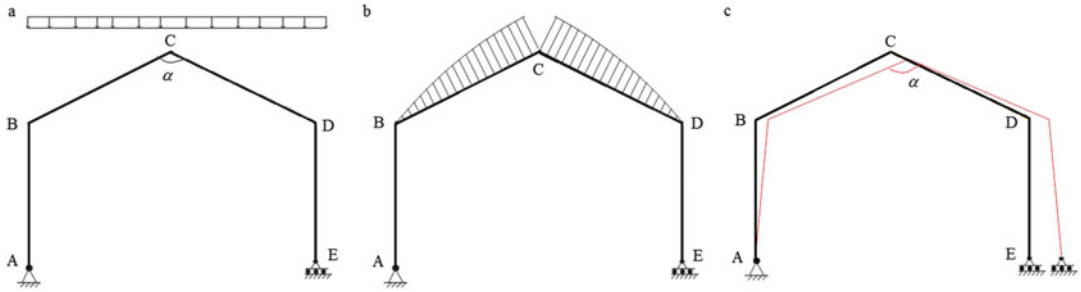

Fig. 4.29 Simply supported gable frame. (**a**) Loading. (**b**) Bending moment. (**c**) Deflection profile

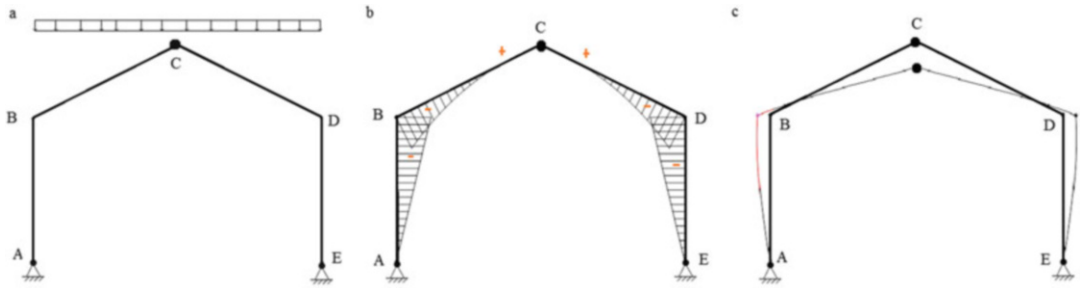

Fig. 4.30 3-Hinge gable frame. (**a**) Loading. (**b**) Bending moment. (**c**) Deflection profile

The examples presented so far have involved gravity loading. Lateral loading is treated in a similar way. One first determines the moment diagrams, and then establishes the curvature patterns for each member. Lateral loading generally produces lateral displacements as well as vertical displacements. Typical examples are listed below (Figs. 4.31, 4.32, and 4.33).

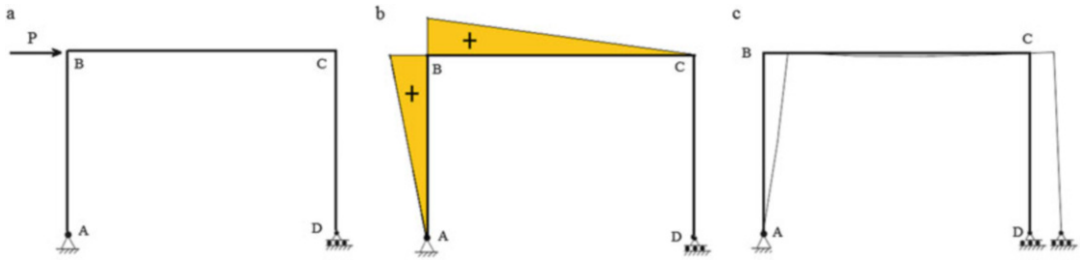

Fig. 4.31 Portal frame. (**a**) Loading. (**b**) Bending moment. (**c**) Deflection profile

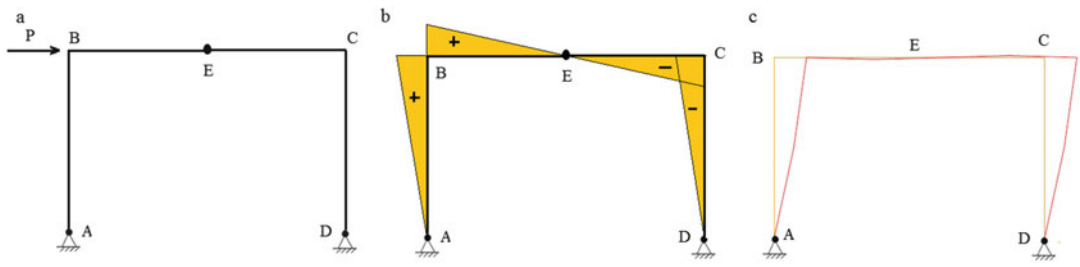

Fig. 4.32 3-Hinge frame. (**a**) Loading. (**b**) Bending moment. (**c**) Deflection profile

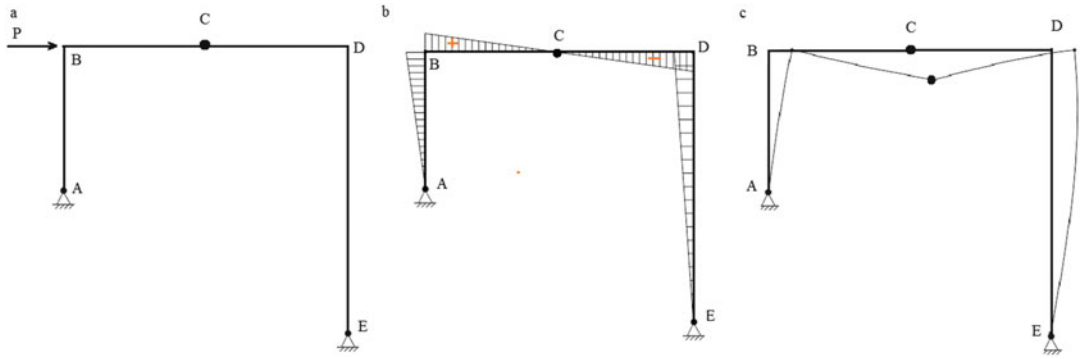

Fig. 4.33 3-Hinge frame. (**a**) Loading. (**b**) Bending moment. (**c**) Deflection profile

4.8 Computer-Based Analysis: Plane Frames

When there are multiple loading conditions, constructing the internal force diagrams and displacement profiles is difficult to execute manually. One generally resorts to computer-based analysis methods specialized for frame structures. The topic is discussed in Chap. 12. The discussion here is intended to be just an introduction.

Consider the gable plane frame shown in Fig. 4.34. One starts by numbering the nodes and members, and defines the nodal coordinates and member incidences. Next, one specifies the nodal constraints. For plane frames, there are two coordinates and three displacement variables for each node (two translations and one rotation). Therefore, there are three possible displacement restraints at a node. For this structure, there are two support nodes, nodes 1 and 5. At node 1, the X and Y translations are fully restrained, i.e., they are set to zero. At node 5, the Y translation is fully restrained.

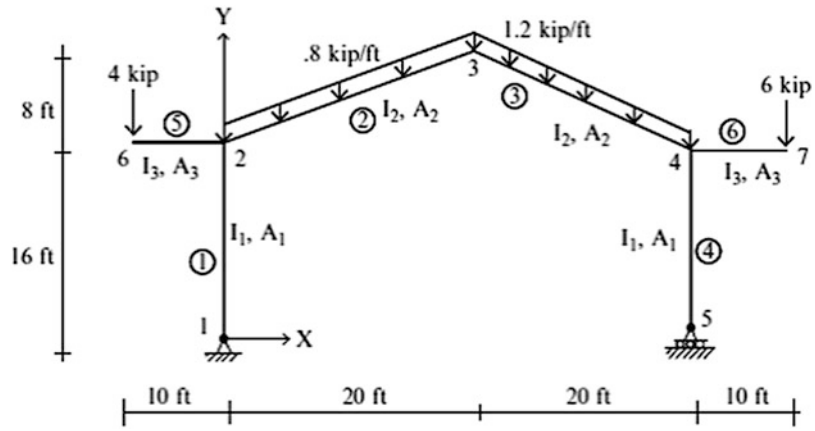

Fig. 4.34 Geometry and loading

Next, information related to the members, such as the cross-sectional properties (A, I), loading applied to the member, and releases such as internal moment releases are specified. Finally, one specifies the desired output. Usually, one is interested in shear and moment diagrams, nodal reactions and displacements, and the deflected shape. Graphical output is most convenient for visualizing the structural response. Typical output plots for the following cross-sectional properties $I_1 = 100$ in.^{4}, $I_2 = 1000$ in.^{4}, $I_3 = 300$ in.^{4}, $E = 29{,}000$ ksi, $A_1 = 14$ in.^{2}, $A_2 = 88$ in.^{2}, and $A_3 = 22$ in.^{2} are listed in Fig. 4.35.

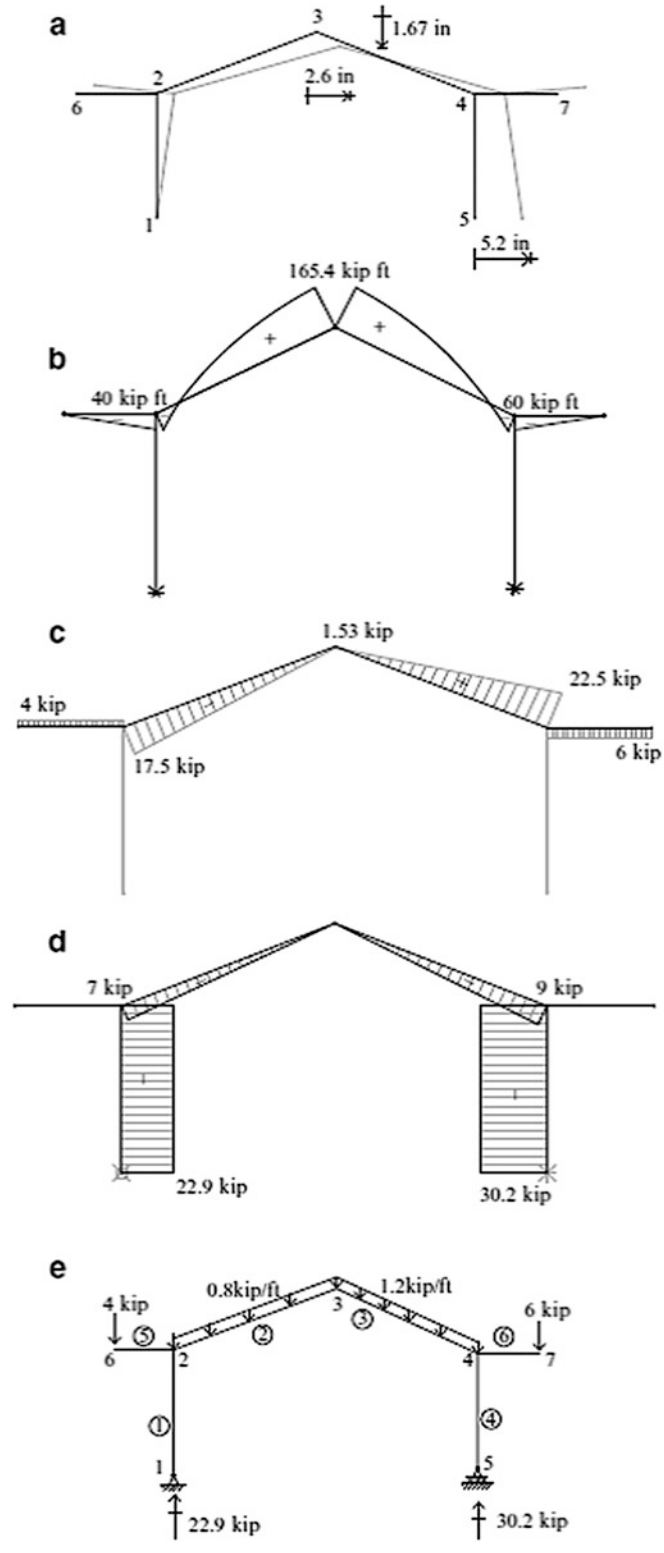

Fig. 4.35 Graphical output for structure defined in Fig. 4.34. (**a**) Displacement profile. (**b**) Bending moment, M. (**c**) Shear, V. (**d**) Axial force, F. (**e**) Reactions

4.9 Plane Frames: Out of Plane Loading

Plane frames are generally used to construct three-dimensional building systems. One arranges the frames in orthogonal patterns to form a stable system. Figure 4.36 illustrates this scheme. Gravity load is applied to the floor slabs. They transfer the load to the individual frames resulting in each frame being subjected to a planar loading. This mechanism is discussed in detail in Chap. 15.

Our interest here is the case where the loading acts normal to the plane frame. One example is the typical highway signpost shown in Fig. 4.37. The sign and the supporting member lie in a single plane. Gravity load acts in this plane. However, the wind load is normal to the plane and produces a combination of bending and twisting for the vertical support. One deals separately with the bending and torsion responses and then superimposes the results.

The typical signpost shown in Fig. 4.37 is statically determinate. We consider the free body diagram shown in Fig. 4.38. The wind load acting on the sign produces bending and twisting moment in the column. We use a double-headed arrow to denote the torsional moment.

Suppose the Y displacement at C is desired. This motion results from the following actions:

Member BC bends in the $X - Y$ plane

$$v_{\mathrm{C}} = \frac{P_{\mathrm{w}}\left(\frac{b}{2}\right)^3}{3EI_2}$$

Member AB bends in the $Y - Z$ plane and twists about the Z axis

$$v_{\mathrm{B}} = \frac{P_{\mathrm{w}}h^3}{3EI_1} \quad \theta_{\mathrm{B}z} = \frac{P_{\mathrm{w}}\left(\frac{b}{2}\right)h}{GJ}$$

where GJ is the torsional rigidity for the cross section.

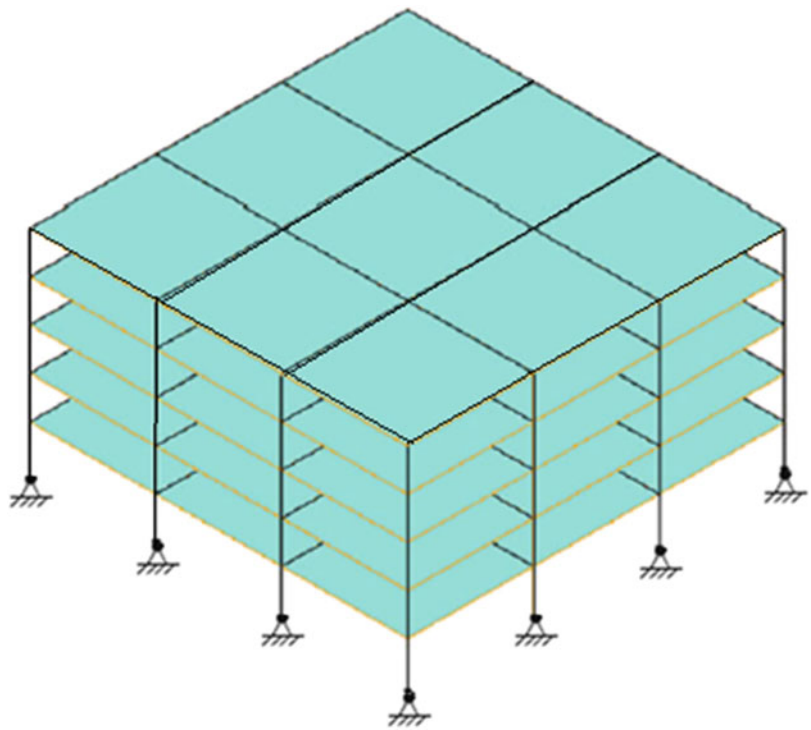

Fig. 4.36 A typical 3-D system of plane frames

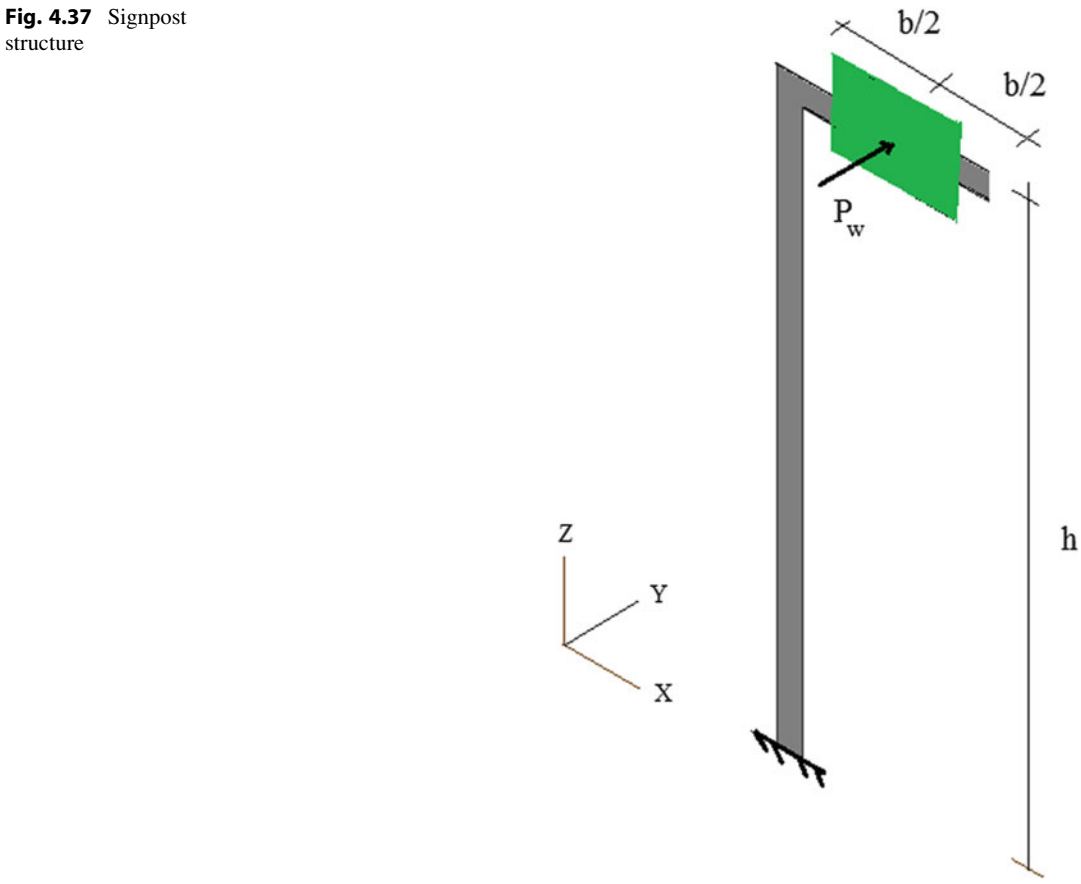

Fig. 4.37 Signpost structure

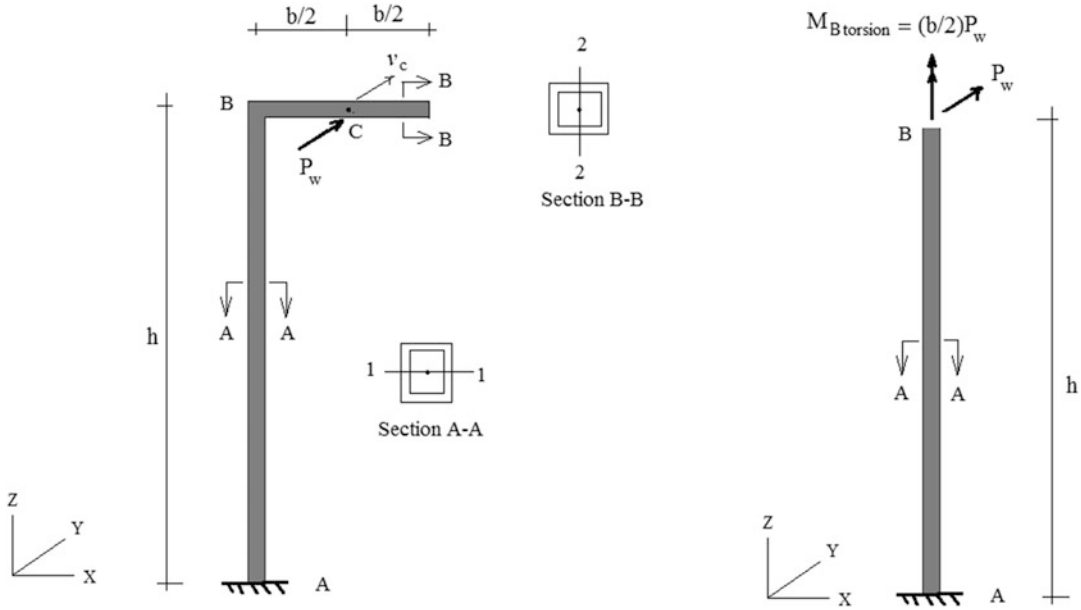

Fig. 4.38 Free body diagrams

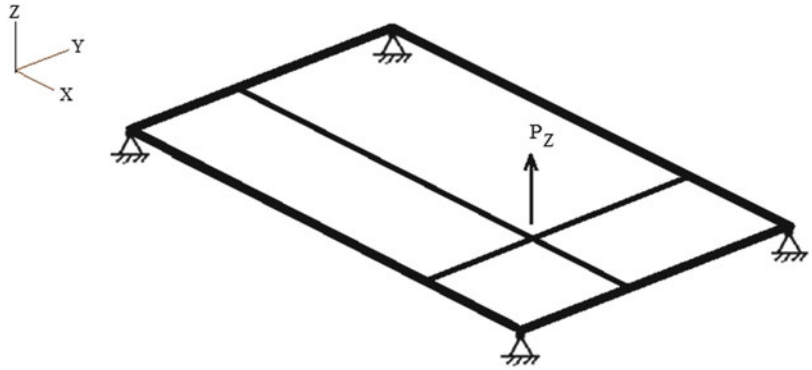

Fig. 4.39 Plane grid structure

Node C displaces due to the rotation at B

$$v_{\mathrm{C}} = \left(\frac{b}{2}\right)\theta_{\mathrm{Bz}} = \left(\frac{b}{2}\right)^2\left(P_{\mathrm{w}}\frac{h}{GJ}\right)$$

Summing the individual contributions leads to

$$v_{\mathrm{c\,total}} = P_{\mathrm{w}}\left(\frac{b^3}{24EI_2} + \frac{h^3}{3EI_1} + \frac{b^2h}{4GJ}\right)$$

Another example of out-of-plane bending is the transversely loaded grid structure shown in Fig. 4.39. The members are rigidly connected at their ends and experience, depending on their orientation, bending in either the $X - Z$ plane or the $Y - Z$ plane, as well as twist deformation. Plane grids are usually supported at their corners. Sometimes, they are cantilevered out from one edge. Their role is to function as plate-type structures under transverse loading.

Plane grids are *statically indeterminate* systems. Manual calculations are not easily carried out for typical grids so one uses a computer analysis program. This approach is illustrated in Chap. 10.

4.10 Summary

4.10.1 Objectives

- To develop criteria for static determinacy of planar rigid frame structures.
- To develop criteria for static determinacy of planar A-frame structures.
- To present an analysis procedure for statically determinate portal and pitched roof plane frame structures subjected to vertical and lateral loads.
- To compare the bending moment distributions for simple vs. 3-hinged portal frames under vertical and lateral loading.
- To describe how the Principle of Virtual Forces is applied to compute the displacements of frame structures.
- To illustrate a computer-based analysis procedure for plane frames.
- To introduce the analysis procedure for out-of-plane loading applied to plane frames.

4.10.2 Key Concepts

- A planar rigid frame is statically determinate when $3\,m + r - n = 3j$, where m is the number of members, r is the number of displacement restraints, j is the number of nodes, and n the number of releases.
- A planar A-frame is statically determinate when $3\,m = r + 2n_{\mathrm{p}}$, where n_{p} is the number of pins, m is the number of members, and r is the number of displacement restraints.
- The Principle of Virtual Forces specialized for frame structures has the general form

$$d\,\delta P = \sum_{\text{members}} \int_s \left\{ \frac{M}{EI}\delta M + \frac{F}{AE}\delta F \right\} \mathrm{d}s$$

  For low-rise frames, the axial deformation term is negligible.
- The peak bending moments in 3-hinged frames generated by lateral loading are generally less than for simple portal frames.

4.11 Problems

For the plane frames defined in Problems 4.1–4.18, determine the reactions, and shear and moment distributions.

Problem 4.1

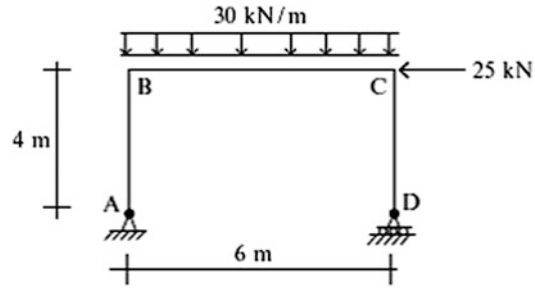

Problem 4.2

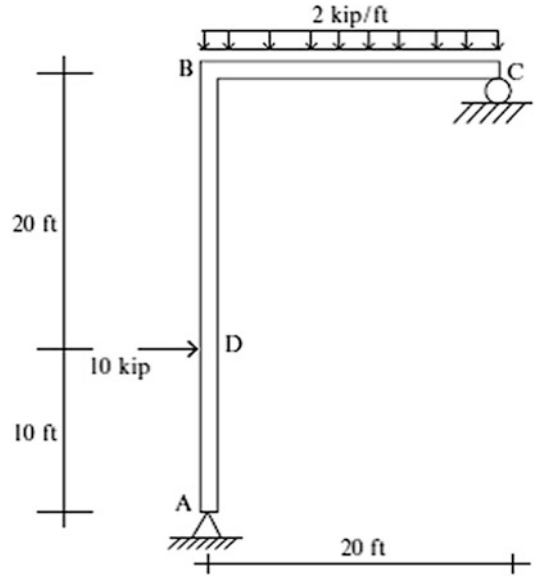

Problem 4.3

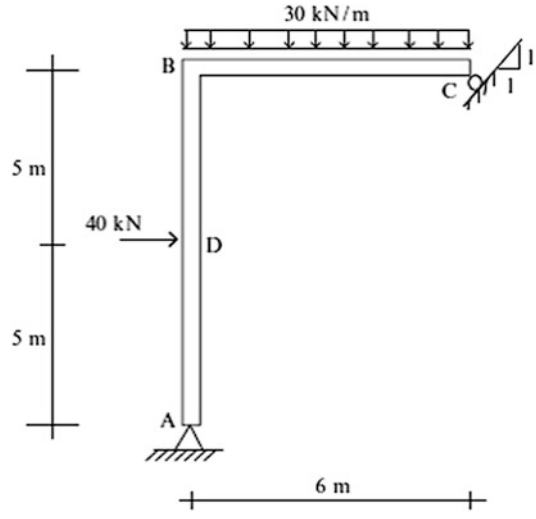

Problem 4.4

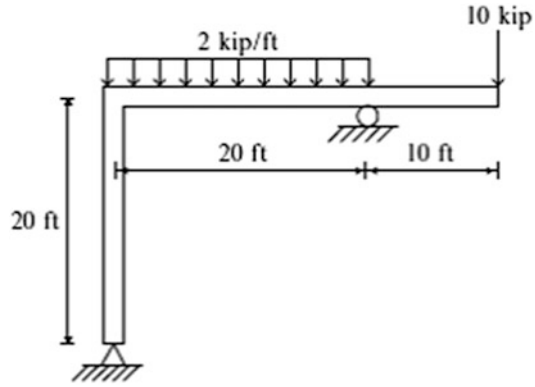

Problem 4.5

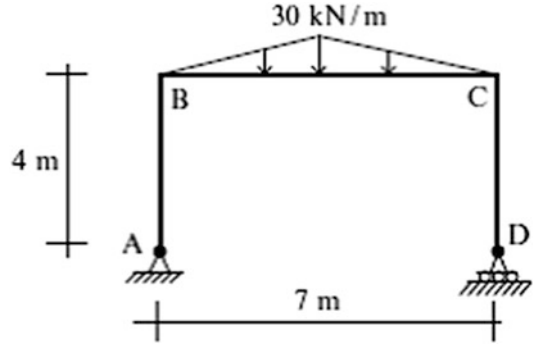

Problem 4.6

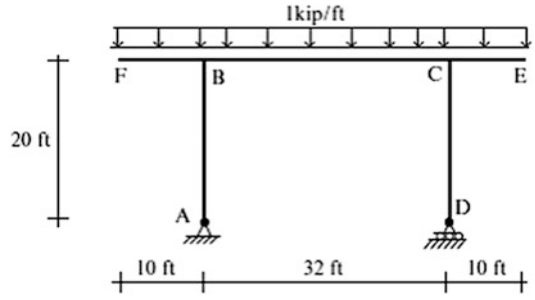

Problem 4.7

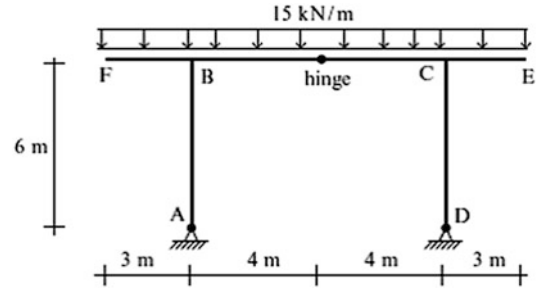

Problem 4.8

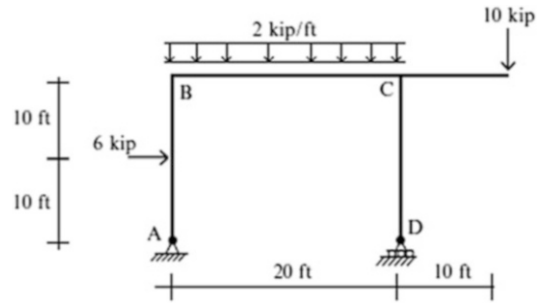

Problem 4.9

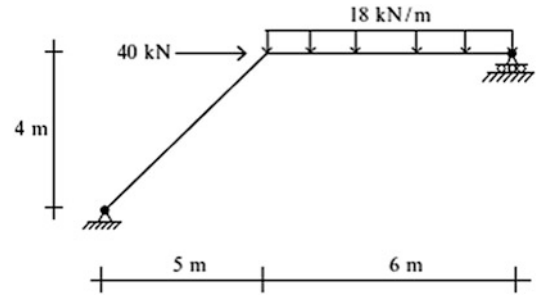

Problem 4.10

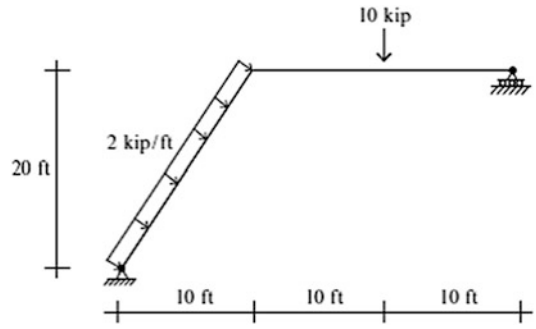

Problem 4.11

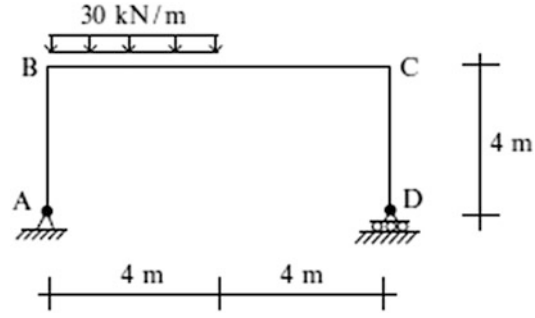

Problem 4.12

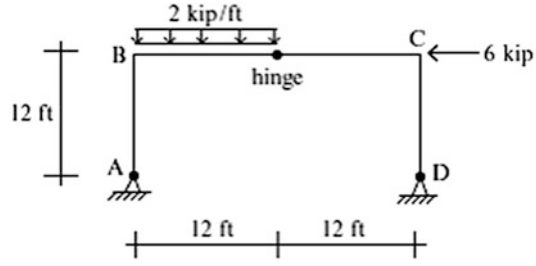

Problem 4.13

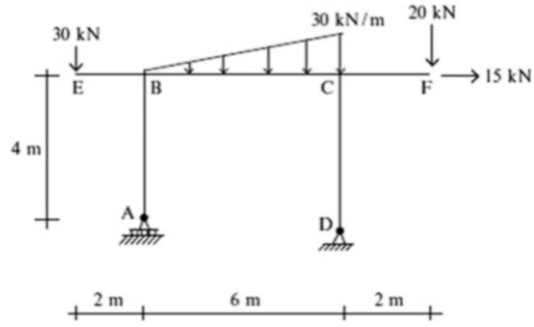

Problem 4.14

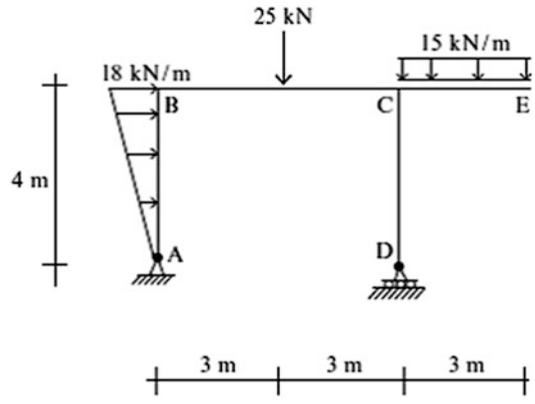

Problem 4.15

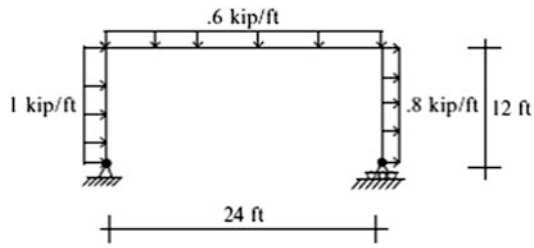

Problem 4.16

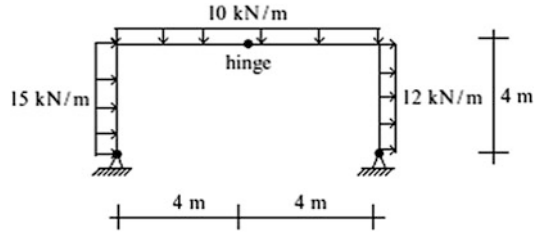

Problem 4.17

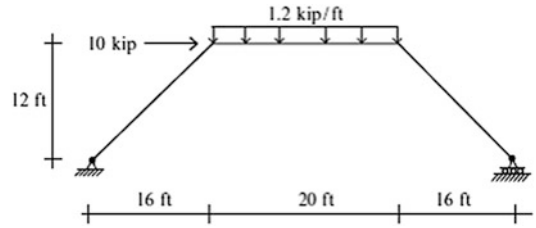

Problem 4.18

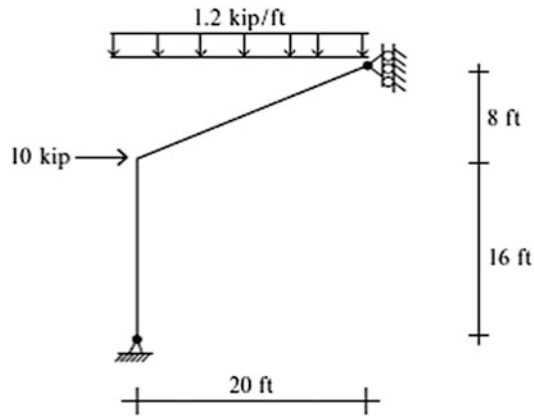

For the gable frames defined in Problems 4.19–4.26, determine the bending moment distributions.

Problem 4.19

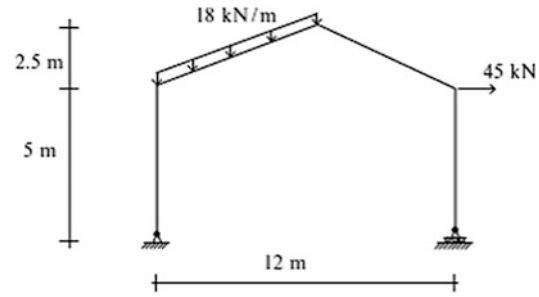

Problem 4.20

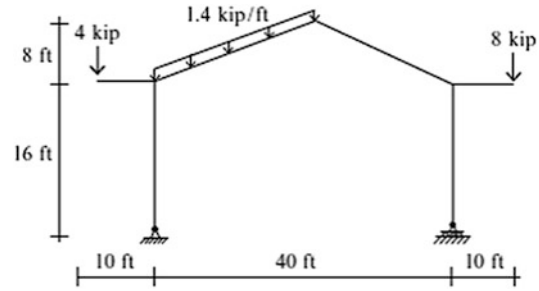

Problem 4.21

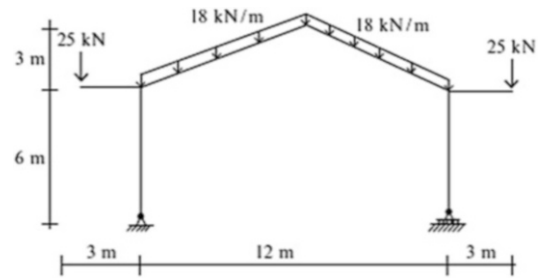

Problem 4.22

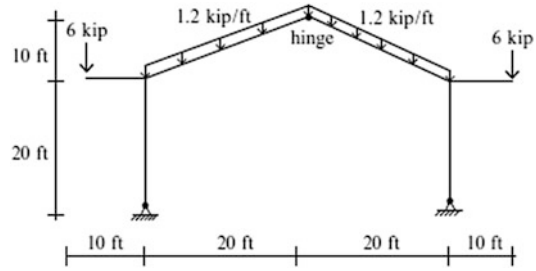

Problem 4.23

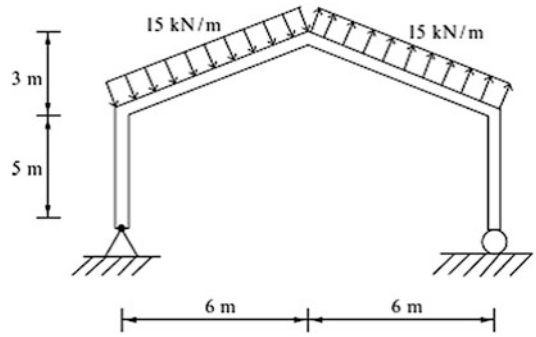

Problem 4.24

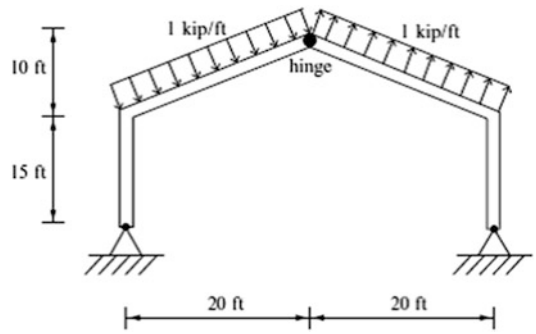

Problem 4.25

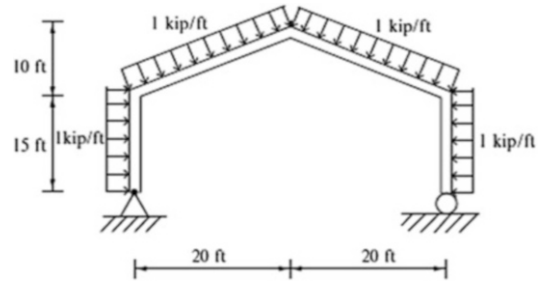

Problem 4.26

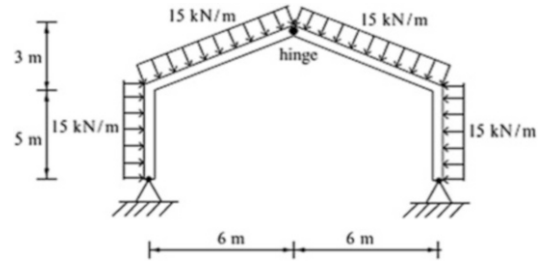

For the A-frames defined in Problems 4.27–4.29, determine the reactions and bending moment distribution.

Problem 4.27

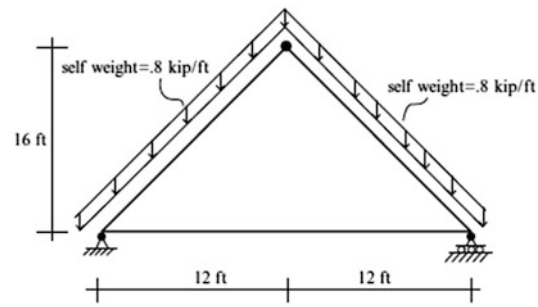

Problem 4.28

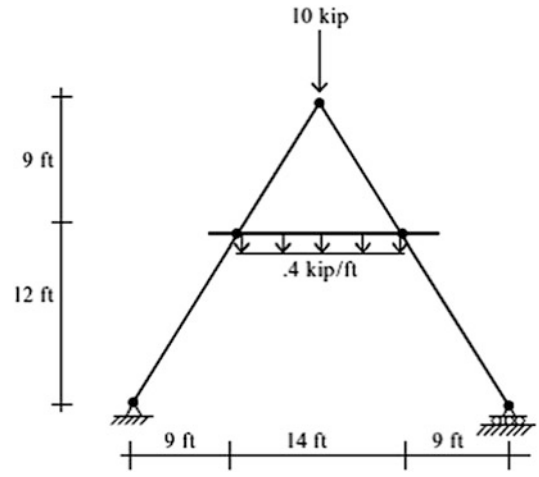

Problem 4.29

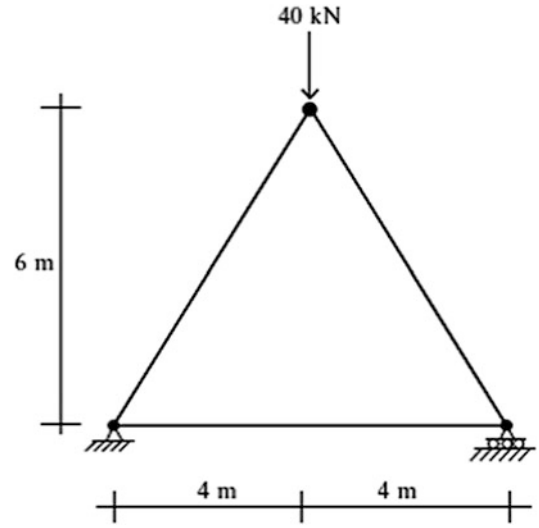

Problem 4.30 Determine the horizontal deflection at D and the clockwise rotation at joint B. Take $E = 29{,}000$ ksi. Determine the I required to limit the horizontal displacement at D to 2 in. Use the Virtual Force method.

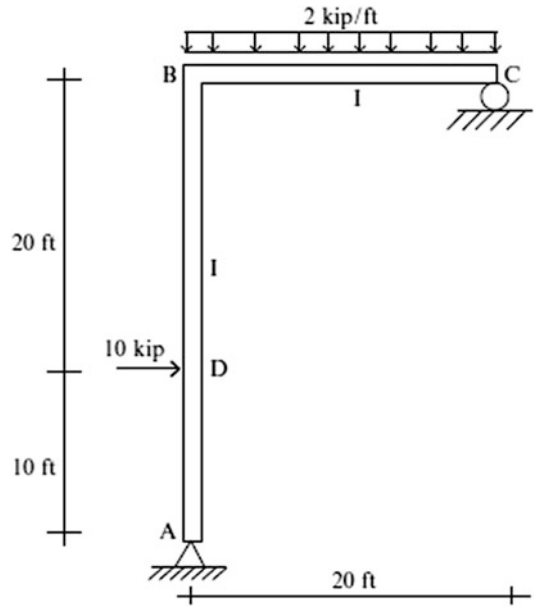

Problem 4.31 Determine the value of I to limit the vertical deflection at C to 30 mm. Take $E = 200$ GPa. Use the Virtual Force method.

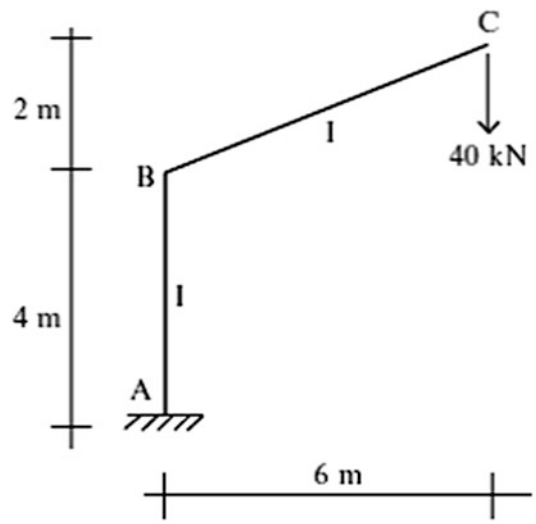

Problem 4.32 Determine the value of I required limiting the horizontal deflection at D to ½ in. Take $E = 29{,}000$ ksi. Use the Virtual Force method.

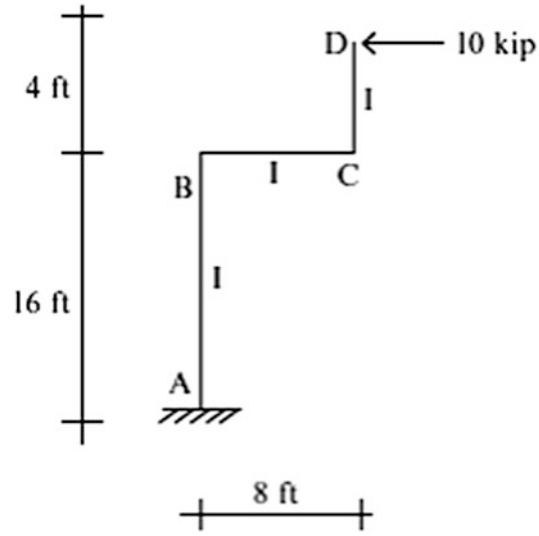

Problem 4.33 Determine the vertical deflection at D and the rotation at joint B. Take $E = 200$ GPa and $I = 60(10)^6$ mm^4. Use the Virtual Force method.

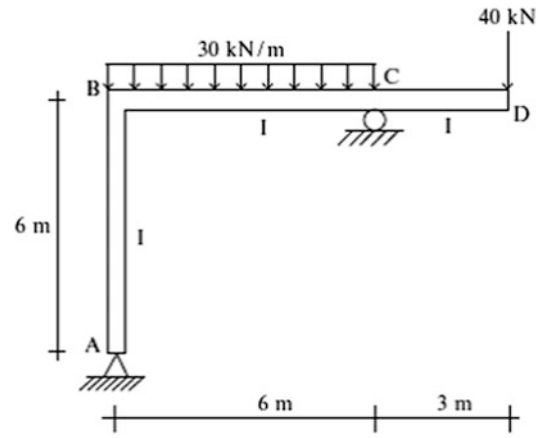

Problem 4.34 Determine the horizontal displacement at joint B. Take $E = 29{,}000$ ksi and $I = 200$ in.^{4} Use the Virtual Force method.

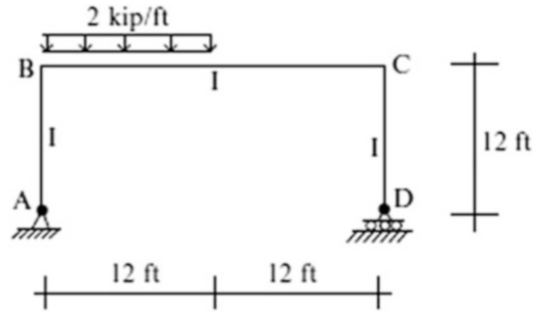

Problem 4.35 Determine the displacement at the roller support C. Take $E = 29{,}000$ ksi and $I = 100$ in.^{4} Use the Virtual Force method.

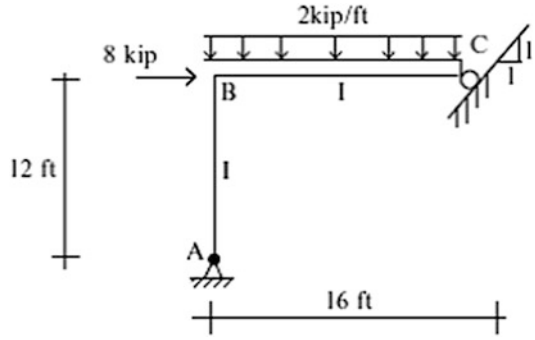

Problem 4.36 Determine the horizontal deflection at C and the rotation at joint B. Take $E = 200$ GPa and $I = 60(10)^6$ mm^4. Use the Virtual Force method.

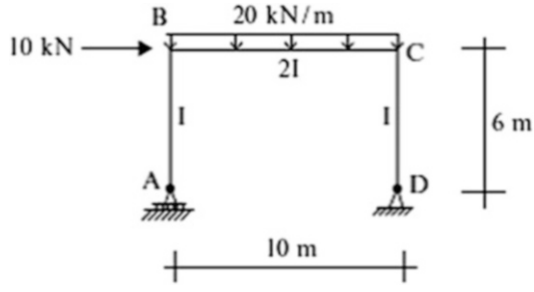

Problem 4.37 Determine the horizontal deflection at C and the vertical deflection at E. Take $E = 29{,}000$ ksi and $I = 160$ in.^{4} Use the Virtual Force method.

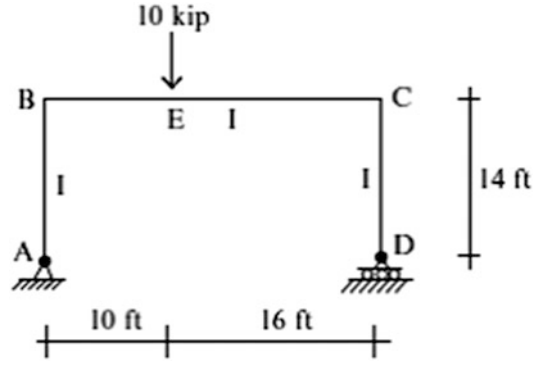

Problem 4.38 Determine the horizontal deflection at C. $I = 100(10)^6$ mm^4 and $E = 200$ GPa. Sketch the deflected shape. Use the Virtual Force method.

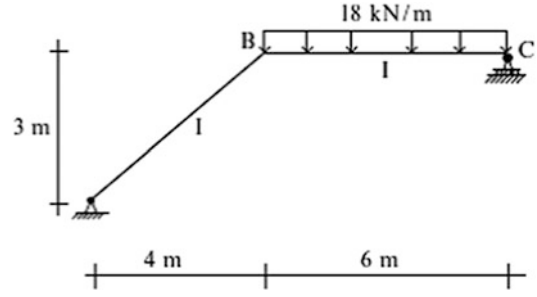

Problem 4.39 Sketch the deflected shapes. Determine the vertical deflection at A. Take $I = 240$ in.^{4}, $E = 29{,}000$ ksi, and $h = 2b = 10$ ft.

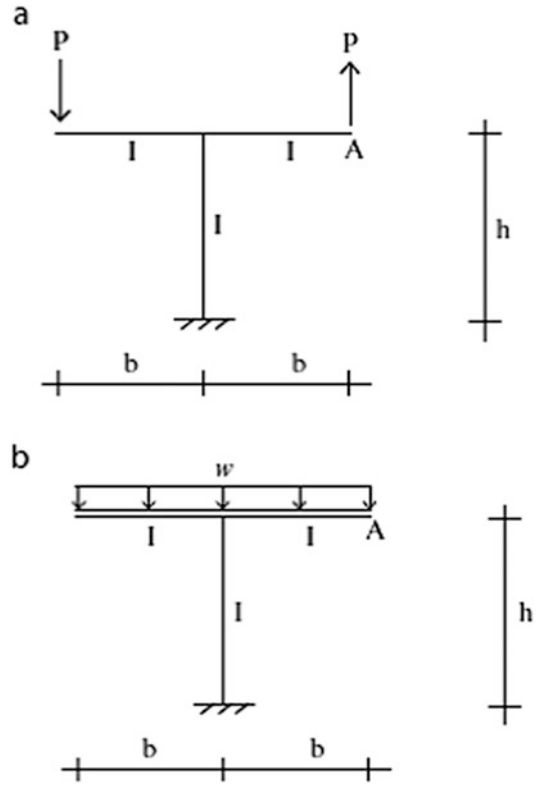

Problem 4.40 Determine the deflection profile for member DBC. Estimate the peak deflection. Use computer software. Note that the deflection is proportional to $1/EI$.

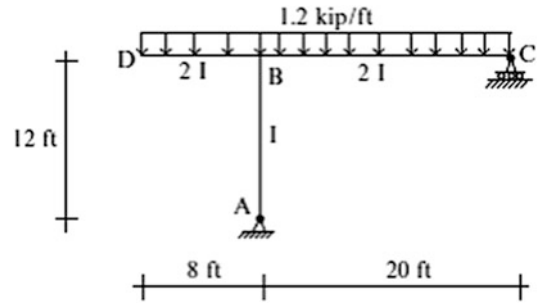

Problem 4.41 Consider the pitched roof frame shown below and the loadings defined in cases (a)–(f). Determine the displacement profiles and shear and moment diagrams. *EI* is constant. Use a computer software system. Take $I = 10{,}000$ in.^{4} ($4160(10)^6$ mm^4), $E = 30{,}000$ ksi (200 GPa).

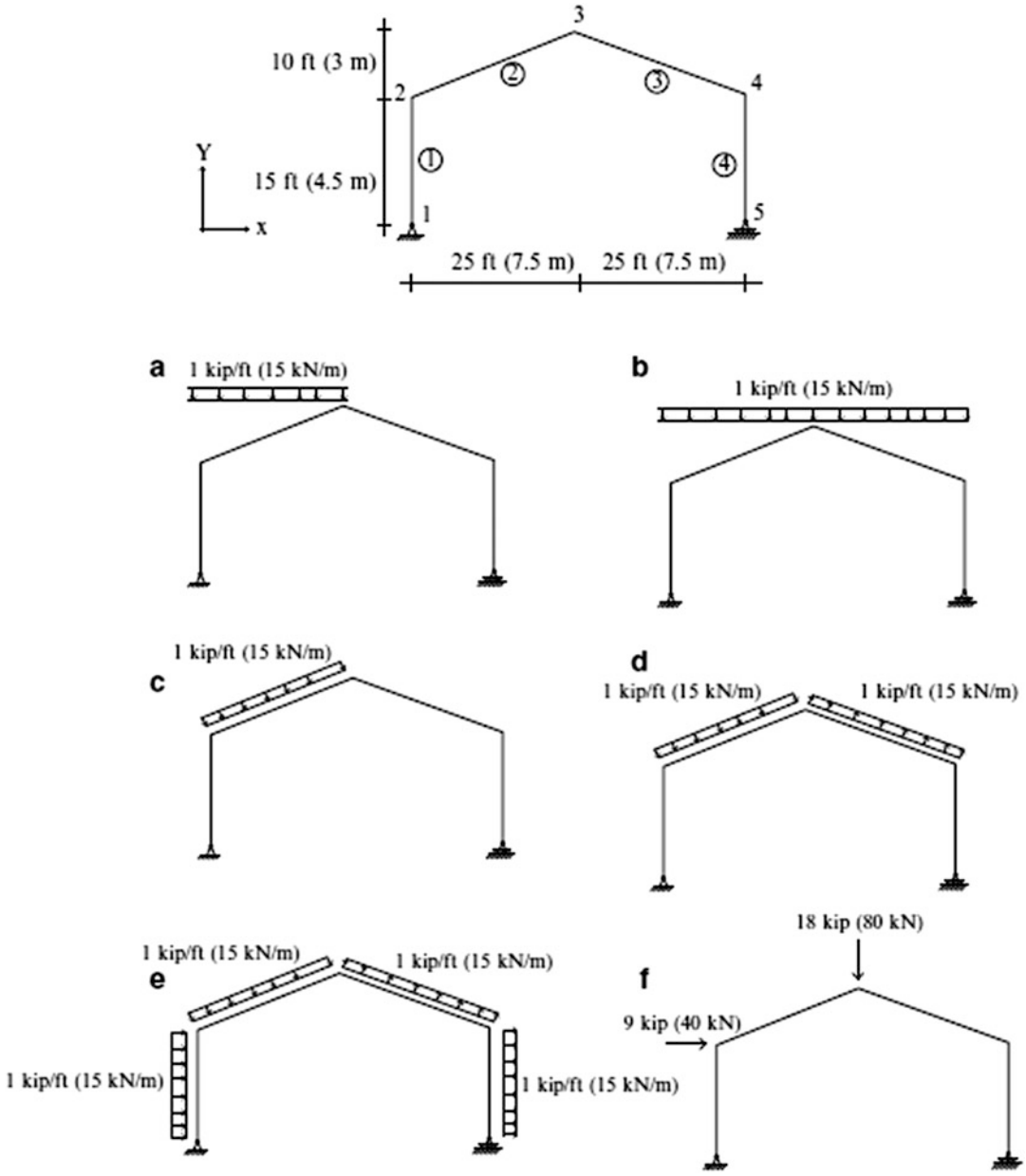

Problem 4.42 Consider the frame shown below. Determine the required minimum I for the frame to limit the horizontal deflection at C to 0.5 in. The material is steel. Use computer software.

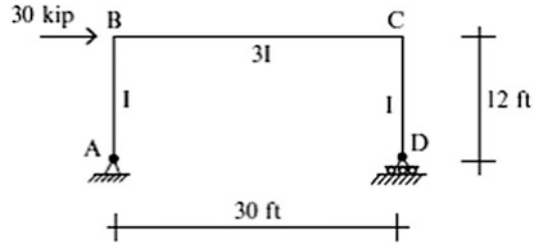

Problem 4.43 Consider the frame shown below. Determine the required minimum I for the frame to limit the vertical deflection at E to 15 mm. The material is steel. Use computer software.

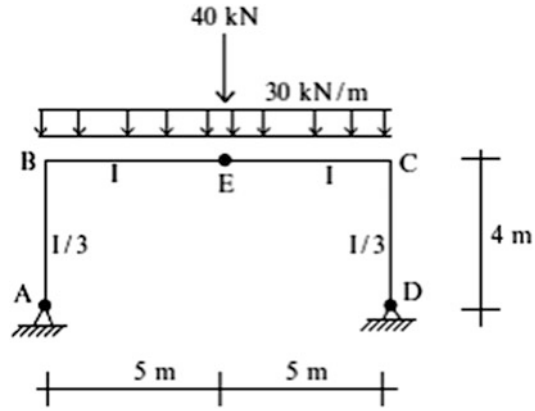

Problem 4.44 Consider the triangular rigid frame shown below. Assume the member properties are constant. $I = 240$ in.^{4}, $A = 24$ in.^{2} and $E = 29{,}000$ ksi. Use computer software to determine the axial forces and end moments for the following range of values of tan $\theta = 2$ $h/L = 0.1, 0.2, 0.3, 0.4, 0.5$

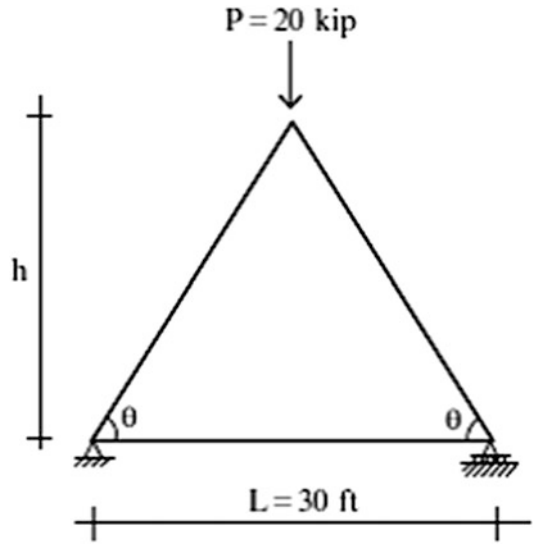

Compare this solution with the solution based on assuming the structure is an ideal truss.

Problem 4.45 Consider the structure consisting of two members rigidly connected at B. The load P is applied perpendicular to the plane ABC. Assume the members are prismatic. Determine θ_y at point C (labeled as θ_c on the figure).

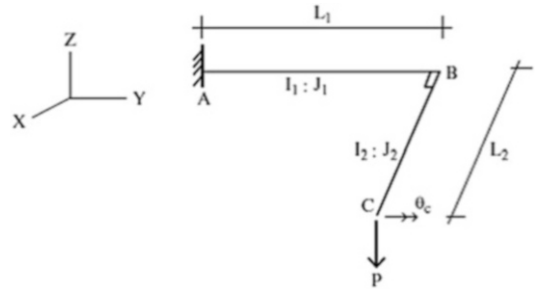

Problem 4.46 Members AB, BC, and CD lie in the $X - Y$ plane. Force P acts in the Z direction. Consider the cross-sectional properties to be constant. Determine the z displacement at B and D. Take $L_{AB} = L, L_{BC} = \frac{L}{2}, L_{CD} = L\sqrt{2}$.

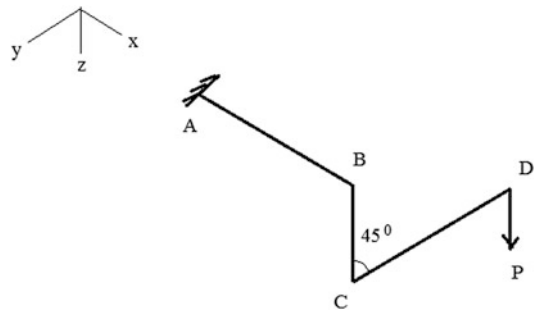

Reference

1. Tauchert TR. Energy principles in structural mechanics. New York: McGraw-Hill; 1974.